A Monte Carlo program for simulating segregation and diffusion utilizing chemical potential calculations

by

Heinrich Daniel Joubert

B.Sc Hons.

a thesis presented in fulfilment of the requirements of the degree

MAGISTER SCIENTIAE

in the Department of Physics

at the University of the Free State

Republic of South Africa

Promoter: **Dr J.J. Terblans**

Co-promoter: **Prof H.C. Swart**

May 2004

For my parents

Anton & Sophie

Acknowledgements

The author wishes to express his thanks and gratitude to the following people:

- *My parents,* for their unending love and support
- *My promoters,* for all their patience and support during this study
- *The National Research Foundation,* for financial assistance
- *The personnel of the Physics Department*, for numerous informative conversations
- *Mr E. Wurth,* for all his assistance with the temperamental computers

Key words

Atomic concentration
Diffusion
Chemical potential
Change in chemical potential
Modified Darken model
Fick’s model
Monte Carlo Method
Segregation
Segregation energy

Abstract

Bulk-to-surface segregation plays a major role in the engineering of alloy surfaces. An increase in surface sensitive analysis techniques in recent years have led to big advances in the engineering of surface properties. The focus of this study is the development of a *Chemical Potential Monte Carlo* (CPMC) model which is based on the modified Darken model. This model is capable of simulating diffusion and segregation in crystals with a uniform concentration as well as crystals consisting of thin layers.

The chemical potential equations used for the calculations by the modified Darken model are rewritten to include the segregation energy associated with the surface layer. The change in chemical potential directs atomic motion and simulations involving the change in chemical potential are performed on a 2-dimensional matrix containing two elements: the solute and the solvent elements.

A random selection of an atom inside the matrix initiates the model. The change in chemical potential due to an atomic jump of a randomly selected atom to an adjacent layer is calculated. The largest change in chemical potential directs the atomic motion, complying with the conditions associated with the lowering of the Gibbs free energy; the driving force of atomic motion is therefore the lowering of the total crystal energy. Inclusion of the segregation energy (for jumps involving the surface layer) limits the number of atomic jumps from the surface layer to the bulk.

Simulated segregation profiles generated by the CPMC model were compared with profiles calculated with both the modified Darken and Fick model. The comparisons show that the CPMC successfully describes both the kinetic and equilibrium conditions associated with surface segregation. A reduction in calculation time was also achieved by implementing the CPMC model in parallel.

Table of Contents

Chapter 1

Introduction

The surface-segregation phenomenon is one of the most fascinating and important processes that influence the engineering of materials' surfaces. When a surface of an alloy (or catalyst) can be engineered to possess certain properties, the uses of the alloy increase dramatically. A typical example is the catalytic converters used to clean the exhaust gas of motor vehicles [1]. The effectiveness of the catalyst depends on the surface composition of the catalytic surface. Impurities that adsorb onto the surface lower the effectiveness and life-expectancy of the catalyst. To improve the efficiency of the catalyst, certain elements are added to the bulk composition [1]. These elements segregate to the surface as a result of the adsorption of atoms onto the catalytic surface. The addition of such elements increases the life-expectancy and efficiency of the catalyst dramatically.

Experimental investigation of surface-segregation has increased over the last few decades with the development of surface sensitive analysis techniques such as Auger Electron Spectroscopy [2]. With these techniques the surface of the sample under investigation can be monitored and the segregation effect recorded. Models that describe and explain the segregation process were also developed to augment experimental measurements [2]. Two of the best known models are the infinite solution of Fick's first law (which describes the kinetics of segregation for a short period of time) and the Langmuir-

McLean equation that describes the equilibrium condition associated with surface segregation [2]. A lesser known segregation model is the modified Darken model [2] which is capable of simulating both the kinetic and equilibrium conditions for segregation. All three models are discussed in Chapter 4.

In addition to the models mentioned above, diffusion and segregation models that utilize the Monte Carlo Method are receiving more attention as computing power increases. As an example, Czerwinski, et. al. [13] employed a random walk method to simulate the diffusion of Ni through both the grain boundaries and the lattice of NiO at high temperatures and Deng, et. al. [26] used the Monte Carlo Method to simulate surface segregation in Pt-Pd and Pt-Ir alloys with an embedded-atom method. The modified Darken model has been proven to accurately simulate segregation [2] and this study will focus on the development of a Monte Carlo model that is based on the modified Darken model.

Although the modified Darken model is efficient at describing the surface-segregation, it has one major drawback: it utilizes many differential equations that must be solved simultaneously. The solution of these equations requires extensive computing power and time [2]. Often when calculations require a lot of computing time, the calculations are performed in parallel. However, the way the modified Darken model works (simultaneous solution of many differential equations) means that it is very difficult to implement in parallel [2].

In an effort to decrease the total calculation time, a Chemical Potential Monte Carlo (CPMC) model was developed. The CPMC model rapidly produces surface-segregation profiles which can be added together to improve the statistics of the profile. The CPMC model is based on the proven modified Darken model and it is capable of simulating segregation by using chemical potential calculations, similar to the modified Darken model [2,3]. The CPMC model is not intended to replace the modified Darken model.

Instead it can be used in conjunction with the modified Darken model and also when speedy theoretical modelling of segregation is needed.

1.1 Purpose of this study

This study's main focus is the development of a theoretical segregation model that is easily implemented in a parallel processing environment. At this stage the model simulates segregation in binary alloys, but the nature of the model allows easy extension to ternary and higher order alloys. The CPMC model's design also allows thin film studies to be conducted, but the focus of this study will be on crystals with a uniform concentration.

1.2 Layout of the thesis

Chapter 2 introduces the reader to the theory behind the Monte Carlo Method. The properties and types of random variables are discussed. Also, random number generators are discussed.

Chapter 3 discusses the theory of diffusion and explains Fick's diffusion laws. A typical example of the implementation of the Monte Carlo Method is also briefly discussed.

Chapter 4 focuses on the general theory of segregation. It is shown that Fick's diffusion laws describe the kinetic part of segregation but it fails to describe the equilibrium condition predicted by the Langmuir-McLean equation. This can be attributed to the way in which Fick's laws describe diffusion: movement of atoms from an area of high concentration to an area of low concentration. The modified Darken model discussed in

the chapter relies on the reduction of the total crystal energy as the driving force behind segregation, which is why the modified Darken model describes both the kinetic and equilibrium situations of segregation correctly.

Chapter 5 introduces a Chemical Potential Monte Carlo model based on the modified Darken model of segregation. This model uses the Monte Carlo Method in conjunction with chemical potential calculations to simulate atomic motion. The driving force, similar to the Darken model, is the reduction of the total crystal energy. This is achieved by calculating the change in chemical potential, where the largest positive change in chemical potential directs atomic motion.

Chapter 6 discusses the results obtained with the Chemical Potential Monte Carlo model and compares the results with Fick's model as well as the modified Darken model.

A brief conclusion is given in *Chapter 7*.

Chapter 2

Introduction to the Monte Carlo Method

2.1 Introduction

The Monte Carlo Method is a statistical technique utilizing random quantities to find approximate solutions of mathematical or physical problems

This chapter serves as the foundation for the model described in Chapter 5. Before any study employing the Monte Carlo Method can be attempted, a few basic properties of random variables and random number generators must be discussed.

With the advent of modern computers in the first half of the 20^{th} century, the Monte Carlo Method evolved into a powerful numerical technique with wide ranging applications in scientific circles. This chapter describes the origin of the Monte Carlo Method as well as the theory associated with this universal numerical technique.

2.2 The origin of the Monte Carlo Method

The article published by N. Metropolis and S. Ulam in 1949, entitled *"The Monte Carlo Method"*, is widely accepted as the first paper linking the Monte Carlo name to the use of random quantities [6]. This article is by no means the first implementation of random numbers to solve statistical problems. An experiment recorded in the Bible (1 Kings vii. 23 and 2 Chronicles iv. 2) reveals that p was deduced by comparing the circumference and width of columns in King Solomon's temple. Random quantities are certainly not a recent invention.

The "Monte Carlo" name has its origins in the city of Monte Carlo, which became famous for the gambling establishment in the city. Coincidently, a simple way of obtaining random quantities is by using a roulette wheel [6]. A detailed discussion of random number generators follows in later sections of this chapter.

To illustrate the many uses of the Monte Carlo method, a brief description of a basic implementation of the method is discussed: suppose the surface area of a 2-dimensional surface must be determined (Figure 2.1). The 2-dimensional surface S is contained in a unit square of area A. N random points are positioned inside the unit square. The number of points lying inside of S are designated N'. The area can now be determined from the ratio $\frac{N'}{N} \times A$. A larger N leads to increased accuracy in the estimates of the surface area [6].

The Monte Carlo Method is not generally used to find the area of a plane surface; other methods provide greater accuracy. However, the volume of many-dimensional bodies are readily solved with the Monte Carlo Method whereas other techniques are extremely complicated or do not exist [6].

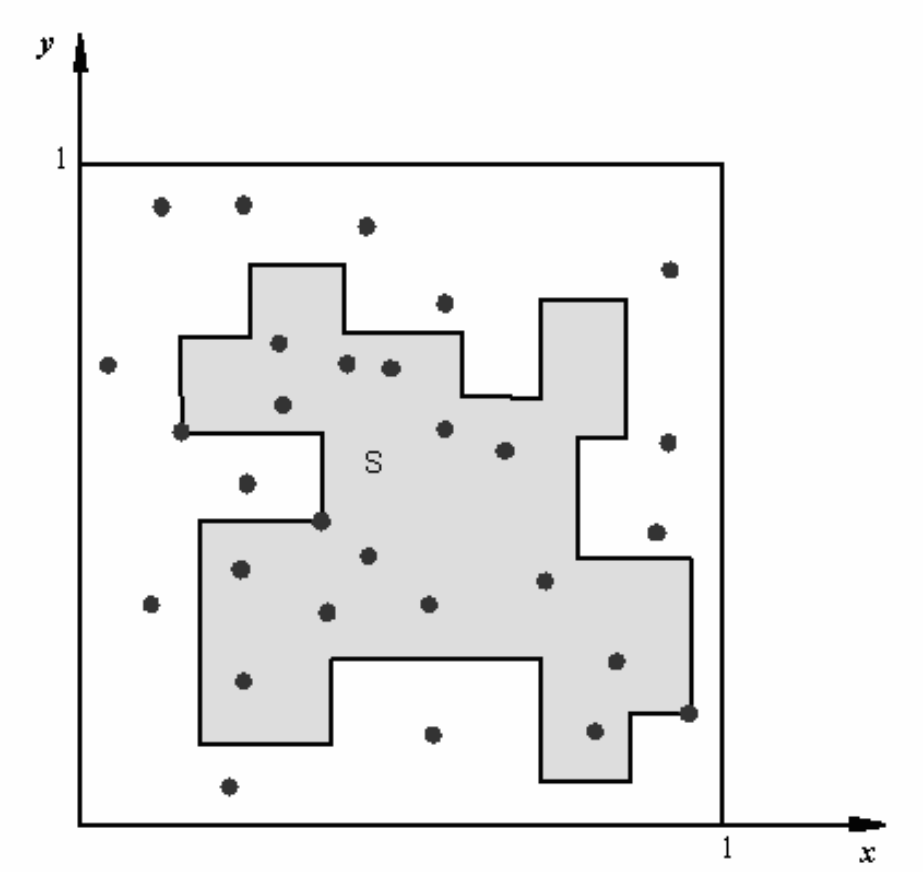

Figure 2.1: Example usage of the Monte Carlo Method to determine the surface area of the surface S

Some examples of the application of the Monte Carlo Method include neutrons diffusing in material [7], radiation shielding, applications in polymer crystals [8] and more recently, applications in neural networks and automated target recognition in modern warfare [9]. The last few decades have seen a dramatic increase in computing power, rendering the Monte Carlo Method one of the most powerful techniques for solving mathematical problems. Since the Monte Carlo Method relies heavily on random numbers, the subject of random variables is discussed in the next section.

2.3 Random variables

When the value of a variable in a given case is not known, but the values it can assume and the probabilities with which it can assume these values are known, the variable is called a *random variable*.

However, it is not possible to predict the value of a single random variable, but it is possible to predict the expected value of the variable when a great number of trials are performed. Therefore the more trials there are, the more accurate the prediction will be. Several types of random variables exist and a few of them are discussed in the sections below.

2.3.1 Discrete random variables

If a random variable (X) is discreet, it can assume any of a discreet set of values $x_1, x_2, ..., x_n$, with n an integer [6]. Expressing this relation mathematically leads to

$$X = \begin{pmatrix} x_1 & x_2 & \cdots & x_n \\ p_1 & p_2 & \cdots & p_n \end{pmatrix}, \tag{2.1}$$

where $x_1, x_2, ..., x_n$ are the possible values of the variable X, and $p_1, p_2, ..., p_n$ are the probabilities corresponding to them. The probability that a random variable has the value x_i (denoted by $P(X = x_i)$) is equal to p_i:

$$P(X = x_i) = p_i . \tag{2.2}$$

Equation (2.1) is often called the distribution of the random variable. The numbers $x_1, x_2, \ldots, x_n$ are arbitrary, however the probabilities $p_1, p_2, \ldots, p_n$ must satisfy two

conditions: (1) all p_i are non-negative ($p_i \geq 0$) and (2) the sum of all p_i equals 1 ($p_1 + p_2 + \ldots + p_n = 1$). The second condition implies that for every event X must assume one of the values $x_1, x_2, \ldots, x_n$.

The mathematical expectation (or the expected value) of the random variable X can now be expressed as follows:

$$E(X) = \sum_{i=1}^{n} x_i p_i . \tag{2.3}$$

Equation (2.3) can also be written in the following form (using $\sum_{i=1}^{n} p_i = 1$):

$$E(X) = \frac{\sum_{i=1}^{n} x_i p_i}{\sum_{i=1}^{n} p_i} . \tag{2.4}$$

From the previous expression it can be seen that $E(X)$ is in a sense the average value of the variable X, in which the more probable values are added into the sum with larger weights. The process of averaging weights is common practice in science, e.g. the abscissa of the center of gravity of a particular system is given by the formula [6]

$$\overline{X} = \frac{\sum_{i=1}^{n} x_i m_i}{\sum_{i=1}^{n} m_i} . \tag{2.5}$$

At this stage it is pertinent to mention some properties of mathematical expectation, since this concept is widely used throughout this chapter. For any constant c, the following expressions are applicable to the mathematical expectation:

$$E(X+c)=E(X)+c, \tag{2.6}$$

$$E(cX)=cE(X). \tag{2.7}$$

If X and Y are any two random variables, then

$$E(X+Y)=E(X)+E(Y). \tag{2.8}$$

It is also possible to find the variance of the random variable X [6]:

$$\mathrm{Var}(X)=E\left(\left(X-E(X)\right)^2\right). \tag{2.9}$$

This variance Var(X) is the mathematical expectation of the squared deviation of the random variable X from its average value $E(X)$. The variance is also always greater than or equal to zero. The variance and the mathematical expectation are the most important numbers used to characterize the random variable X. As an illustration, if a variable X is observed N times, the following values are obtained: $X_1, X_2, \ldots, X_N$, where each of these numbers is equal to one of the numbers $x_1, x_2, \ldots, x_n$. The arithmetic mean of these numbers will then be close to $E(X)$:

$$\frac{1}{N}\left(X_1+X_2+\ldots+X_N\right)\approx E(X), \tag{2.10}$$

while the variance characterizes the spread of these values around the average $E(X)$.

To simplify calculations, equation (2.9) can be transformed using equations (2.6)-(2.8), which lead to

$$\mathrm{Var}(X) = E\left(X^2\right) - \left(E(X)\right)^2. \tag{2.11}$$

As with the mathematical expectation, the variance also possess certain properties: If c is any constant, then

$$\mathrm{Var}(X + c) = \mathrm{Var}(X), \tag{2.12}$$

$$\mathrm{Var}(cX) = c^2 \mathrm{Var}(X). \tag{2.13}$$

Another important concept of random variables is the independence of the variables. To illustrate this concept, two random variables are observed. If the distribution of X does not change when the value that the variable Y assumes is varied, then X and Y do not depend on each other, hence they are independent. The following relations hold for independent variables X and Y:

$$E(XY) = E(X)E(Y), \tag{2.14}$$

$$\mathrm{Var}(X + Y) = \mathrm{Var}(X) + \mathrm{Var}(Y). \tag{2.15}$$

The following example illustrates the use of mathematical expectation and variance:

Example 1: Consider a random variable X with the distribution

$$X = \begin{pmatrix} 1 & 2 & 3 & 4 & 5 & 6 \\ \frac{1}{6} & \frac{1}{6} & \frac{1}{6} & \frac{1}{6} & \frac{1}{6} & \frac{1}{6} \end{pmatrix}.$$

Using equation (2.3), the mathematical expectation is found to be

$$E(X) = \tfrac{1}{6}(1+2+3+4+5+6) = 3.5,$$

which describes the expected value of the random numbers. The variance is found from equation (2.11):

$$\begin{aligned}\mathrm{Var}(X) &= E(X^2) - (E(X))^2 \\ &= \tfrac{1}{6}(1^2+2^2+3^2+4^2+5^2+6^2) - (3.5)^2 \\ &= 2.917.\end{aligned}$$

The variance, in turn, describes the spread of the random variables around the expected value.

2.3.2 Continuous random variables

When a random variable X can assume any value in some interval [a,b], the random variable is said to be continuous.

A function, $p(x)$, assigned to the random variable X in the interval [a,b], describes all the possible values of this variable [6]. This function is known as the density distribution or probability density of the random variable X. The probability that X lies in an arbitrary interval [a',b'] with $(a \le a', b' \le b)$ is given by

$$P(a' < X < b') = \int_{a'}^{b'} p(x)dx. \qquad (2.16)$$

The set of values of X can be any interval. This interval can contain either or both of its endpoints, as well as the case when $a = -\infty$ and $b = \infty$. The density function must also comply with two conditions:

$$p(x) \ge 0, \qquad (2.17)$$

$$\int_a^b p(x)\,dx = 1. \tag{2.18}$$

It is now possible to write down an expression for the expected value of the continuous random variable, similar to the expectation of the discrete random variable [6]:

$$E(X) = \int_a^b xp(x)dx\,. \tag{2.19}$$

Following the same procedure described in the previous section, equation (2.19) can be rewritten as

$$E(X) = \frac{\int_a^b xp(x)dx}{\int_a^b p(x)dx}, \tag{2.20}$$

which is the average value of X. Stated otherwise, the variable X can assume any value of x in the interval (a,b) with weight $p(x)$. The properties of the expectation value as well as the definition of variance described in the previous section are also applicable to continuous random variables.

2.3.3 Normal random variables

A Gaussian (normal) random variable defined in the interval $(-\infty, \infty)$ has a density given by

$$p(x) = \frac{1}{s\sqrt{2p}} \exp\left(-\frac{(x-a)^2}{2s^2}\right) \tag{2.21}$$

where a and $s > 0$ are numerical parameters [6]. a does not affect the shape of the density distribution $p(x)$, it only results in a displacement along the x-axis. s on the other

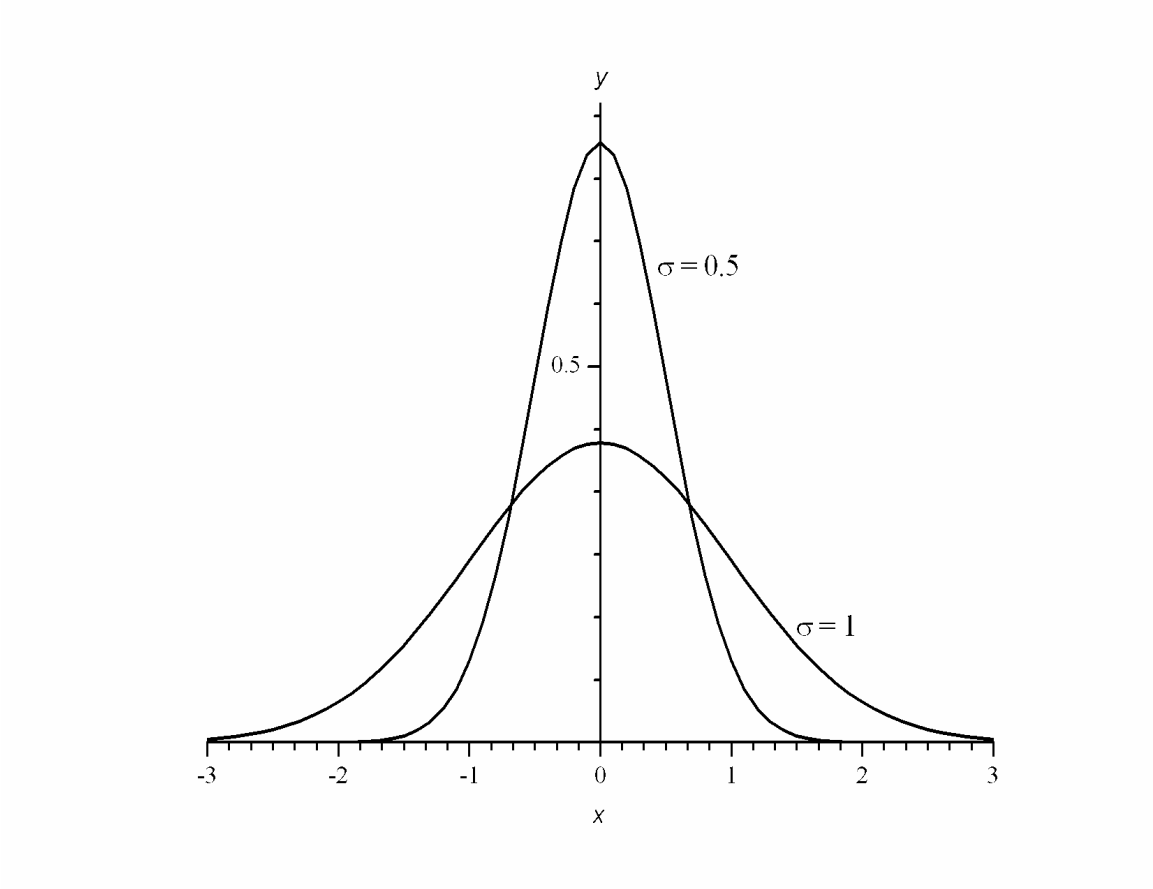

Figure 2.2: Illustration of the influence of *s* on the normal Gaussian distribution.

hand, has a marked influence on the shape of the density distribution. The effect of *s* is illustrated in Figure 2.2.

Applications of random variables are very diverse: an error *d* in measurement is generally a normal random variable. The quantity $s = \sqrt{\mathrm{Var}(d)}$ is called the standard deviation of *d* and it describes the error in the method of measurement. Random variables are definitely one of the most widely used variables in the mathematical sciences today. The properties of random variables described above form an integral part in random number generation, which is discussed in the following section.

2.4 Random number generators

The subject of generating random numbers on a computer often leads to the following questions [6]: *"How can a machine that must be programmed beforehand generate randomness?"* and *"Where did these random numbers come from?"*.

A more correct question [8] is *"Are these numbers correctly distributed?"*. As long as random quantities seem to be randomly drawn from some known distribution, the method of generating the quantities should not affect the person using them [8]. There exist statistical tests to determine the randomness of these numbers, but even these tests have limitations: an infinite amount of tests on an infinite amount of random numbers are needed to ensure that the random numbers satisfy the conditions associated with randomness. Instead of an exhaustive test, a finite number of tests are done on the random numbers; if these tests are satisfied, one assumes that the remaining tests are also satisfied (an example of a simple test is given in the next section).

Generating random numbers become easier if the number of statistical tests that are ignored increase. However, the numbers generated are no longer true random numbers, but rather *pseudo-random* or *quasi-random* [8]. Numbers generated by an equation that imitate the values of a random variable uniformly distributed in [0,1] are called *pseudo-random* numbers [6]. When the generated numbers are more uniformly spread out over their range, a *quasi-random* number sequence is formed [9]. A discussion on how to generate random numbers follows below.

2.4.1 Tables of random numbers

One can easily set up a random number generator by simply removing a random piece of paper from inside a jar or a hat. The values written on the pieces of paper would represent random numbers. A table can then be constructed from the values written on

the pieces of paper. A rotating disc divided into equal parts (each part representing a number) is also an effective random generator. When the disc is suddenly stopped, a fixed arrow indicates the number to be used.

The methods described above have inherent weaknesses, e.g. the pieces of paper in the jar might be statically charged or they might stick to the wall of the jar. To ensure the validity of the numbers generated by these methods, the tables are verified with statistical tests to ensure that no particular characteristics of the group of numbers contradict the hypothesis that the numbers are independent values of a random variable [6]. To illustrate a simple statistical test, consider a table containing N digits. Let the number of zeros in the table be v_0, the number of ones v_1, the number of twos v_2 and so forth. Assuming that the maximum value a random number can assume is nine, the following calculation is performed [6]:

$$\sum_{i=1}^{9} \left(v_i - (0.1)N\right)^2. \tag{2.22}$$

The range in which this sum should lie can be predicted with the theory of probability. This range should not be very large, since the mathematical expectation of each of the v_i is equal to $(0.1)N$. However, it should also not be too small, since this will indicate an overly regular distribution of values.

Tables of random numbers are mostly used when calculations are performed by hand. For calculations utilizing computers, it is more convenient to generate the numbers when needed. Before the subject of mathematical random number generation is discussed, a summary about modular arithmetic is discussed to assist with the understanding of the generators which follow.

2.4.2 Modular Arithmetic

Modular arithmetic was first introduced by Gauss in the 19th century and is a system of arithmetic for certain equivalence classes of integers, called congruence classes, where numbers 'wrap around' after they reach a certain value (the *modulus*). As an example, when the modulus is 12, then any two numbers that leave the same remainder when divided by 12 are equivalent or congruent to each other. The way modular arithmetic is expressed is as follows [10]:

$$a \equiv b \bmod n, \tag{2.23}$$

where a and b are any two numbers and n is called the modulus. Equation (2.23) may be explained as follows: a and b are both in the same congruence class modulo n, i.e., both leave the same remainder on division by n, or, equivalently, $a - b$ is a multiple of n [10]. The value of a can be found by using the relation

$$a = remainder\left(\frac{b}{n}\right). \tag{2.24}$$

To explain the use of modular arithmetic, consider a situation where a 24 hour clock is to be converted to a 12 hour clock.

Let a be the value needed in terms of a 12 hour clock, b the value of a 24 hour clock that must be converted and the modulus n equal to 12:

$$\begin{aligned} a &= 23 \bmod 12 \\ &= remainder\left(\frac{23}{12}\right) \\ &= 11 \end{aligned} \tag{2.25}$$

The value obtained for *a* is the correct value, since 23h00 is equivalent to 11h00 pm. The procedure shown in equation (2.25) is implemented in exactly the same way for the random number generators described below.

2.4.3 Linear congruential generators

This method of generating random numbers uses the generated number to determine the next number [9]. The form of the generator is

$$x_i \equiv \left(ax_{i-1} + c\right) \bmod m, \quad \text{with } 0 \le x_i \le m; \tag{2.26}$$

a is called the multiplier, *c* is called the increment and *m* is called the modulus of the generator. The first value of x_{i-1} used in the calculation (in other words x_0) is called the *seed* value. A multiplicative congruential generator is found when *c* is taken as 0:

$$x_i \equiv \left(ax_{i-1}\right) \bmod m, \quad \text{with } 0 < x_i < m. \tag{2.27}$$

The sequence of numbers generated by equation (2.26) is called a Lehmer sequence [10]. In order to scale the random number sequence into the unit interval [0,1], each x_i is divided by m:

$$u_i = \frac{x_i}{m}. \tag{2.28}$$

With a proper choice of *a* and *m*, the u_i's appear as though they are random and uniformly distributed between 0 and 1.

Since x_i is generated by the preceding x_{i-1}, the maximum period of the linear congruential generator is *m*; the maximum period for a multiplicative generator is *m*-1. As long as the

simulation using the sequence of random numbers completes its calculation within the sequence period, the numbers can be used without patterns emerging.

2.4.4 Multiple recursive generators

Modifying the multiplicative congruential generator leads to a multiplicative recursive generator: by using multiples of a previously generated random number, the next number in the sequence is generated. Expressing this mathematically leads to

$$x_i \equiv \left(a_1 x_{i-1} + a_2 x_{i-2} + \ldots + a_k x_{i-k} \right) \bmod m , \tag{2.29}$$

where k represents a previous number. The advantage of this type of generator is the longer period it has compared to a simple multiplicative generator.

The generators described above are only a few of the generators that are available. For a discussion of other generators, see Gentle, et. al. [10].

2.4.5 Programming languages and random number generators

Most of the popular programming/scientific languages in use today have built in random number generators. These generators do not require the user to set a seed (see section 2.4.3 for an explanation of the seed value) value the first time the generator is run. However, the user has the ability to set the seed if desired. It is also possible to allow the software to choose a seed value by accessing some mechanism such as the system clock. When the generator is invoked after the initial run, the previously generated random number is used as the seed value [10].

When employing several computers to perform the same calculation in parallel, a user-controllable seed becomes an important factor in the calculations. If the initial seed value is the same on all the computers performing the parallel calculations, the results

generated by all the computers will also be the same. These results render the effect of parallel calculations ineffective. If the seed differs from one computer to the next, the negative effect described above disappears. Calculations can then be split between the computers, thus decreasing the total calculation time.

2.5 Diffusion, segregation and the Monte Carlo Method

As mentioned in section 2.1, the advances in computer performance have allowed researchers to develop Monte Carlo models that simulate a vast number of situations. Diffusion and segregation have also been subject to modeling with the aid of the Monte Carlo Method. Most often the Monte Carlo Method is used in conjunction with Finnis-Sinclair type potentials and glue-type potentials, amongst others [11-37]. Several types of Monte Carlo models are also employed to solve diffusion and/or segregation problems. These models include Markov Chain Monte Carlo (also known as the random walk technique), Diffusion Monte Carlo, Kinetic Monte Carlo, Skellerud's Monte Carlo Method and the Metropolis Monte Carlo Method, amongst others [12-37].

With such a large array of applications, the Monte Carlo Method is destined to become a powerful tool for statistical analyses. In the next chapter, the basic theory of diffusion is discussed and an example of a random walk is also briefly discussed.

Chapter 3

Diffusion Theory

3.1 Introduction

Diffusion is a process resulting from random motion of molecules by which there is a net flow of matter that results in the lowering of the total energy. Coincidently this motion is most often from a region of high concentration (high energy) to a region of low concentration (low energy). A familiar example is the perfume of a flower that quickly permeates the still air of a room.

The diffusion process will continue until the total energy of the system is minimized [38], resulting in a uniform distribution of atoms. A typical example of the use of diffusion is in the production of semi-conductors for use in the electronics industry [38]. The segregation models presented in Chapter 4 and 5 all depend on the diffusion of atoms. This chapter serves as a summary of the existing diffusion theory.

3.2 The laws of Fick

Changes in the atomic concentration in a solid can only be achieved through diffusion. There must therefore be a relation between the atomic motion and the diffusion coefficient. The next section provides a derivation of Fick's first law, where a physical meaning is given to the diffusion coefficient in terms of the jump frequency and jump distance of the atoms.

3.2.1 Fick's first law

Consider a crystal where all the diffusing atoms are of the same element, resulting in the diffusion coefficient (*D*) being independent of concentration [43]. Let the concentration of impurity atoms per unit area at position x be N_x and $N_{x+\Delta x}$ at $x+\Delta x$, as shown in Figure 3.1. For this derivation, diffusion is limited to nearest neighbour exchanges.

If an atom jumps G times per second, in other words the mean jump frequency of the atoms is G, then the flux of atoms moving from layer x to layer $x+?x$ is given by [2,43]

$$J_x = \frac{1}{2}\Gamma N_x. \tag{3.1}$$

A similar equation for atoms moving from layer $x+?x$ to x is

$$J_{x+\Delta x} = \frac{1}{2}\Gamma N_{x+\Delta x}. \tag{3.2}$$

From Figure 3.1 and equations (3.1) and (3.2), it follows that the net flux (from $x+\Delta x$ to x) will be

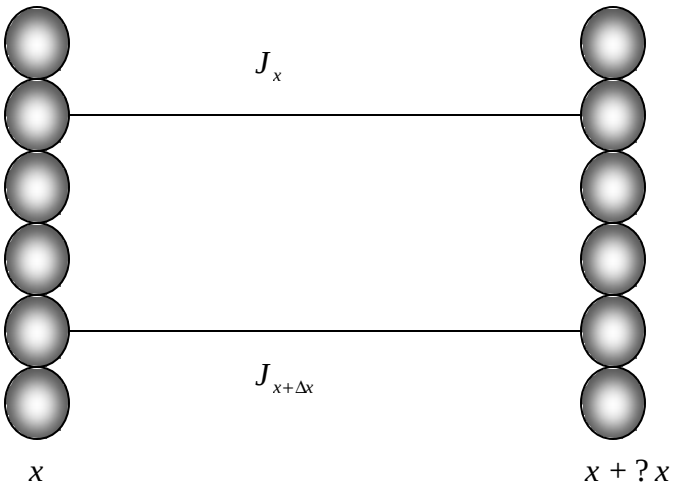

Figure 3.1: Graphical representation of atomic flux used in the derivation of Fick's first law

$$J = J_{x+\Delta x} - J_x = \frac{1}{2}\Gamma(N_{x+\Delta x} - N_x). \tag{3.3}$$

Multiplying equation (3.3) with $\frac{\Delta x^2}{\Delta x^2}$ leads to an expression for the flux in terms of concentration per unit volume and the concentration gradient:

$$\begin{aligned} J &= \frac{1}{2}\Gamma(\Delta x^2)\frac{(N_{x+\Delta x} - N_x)}{\Delta x \Delta x} \\ &= \frac{1}{2}\Gamma(\Delta x^2)\frac{\Delta N}{\Delta x \Delta x}. \end{aligned} \tag{3.4}$$

Replacing $\left(\frac{\Delta N}{\Delta x}\right)$ in equation (3.4) with the concentration ΔC leads to

$$J = -\frac{1}{2}\Gamma(\Delta x)^2 \frac{\partial C}{\partial x} = -D\frac{\partial C}{\partial x} \tag{3.5}$$

with $D = -\frac{1}{2}\Gamma(\Delta x)^2$. Equation (3.5) is Fick's first law [40,43], derived for a one-dimensional setup. If the derivation was done for a 3-dimensional setup, the diffusion coefficient will be [39]

$$D = \frac{1}{6}\Gamma(\Delta x)^2. \tag{3.6}$$

3.2.2 Fick's second law

In most practical situations steady-state conditions are not established. The concentration varies with both distance and time, and Fick's first law can no longer be used. In order to determine how the concentration of atoms at any point in a material varies with time, consider a volume of material with a unit area A and thickness dx, as shown in Figure 3.2.

The number of atoms that diffuse into the volume in a small time interval dt will be $J_1 A dt$ [67]. The number of atoms that leave the volume in the same time interval is $J_2 A dt$. The change in the number of atoms can be expressed as

$$\begin{aligned} \Delta N &= J_1 A dt - J_2 A dt \\ &= (J_1 - J_2) A dt. \end{aligned} \tag{3.7}$$

The concentration of atoms in the volume can be found by dividing ΔN by the volume $A dx$:

$$\begin{aligned} \frac{\Delta N}{A dx} = dC &= \frac{(J_1 - J_2) A dt}{A dx} \\ &= (J_1 - J_2)\frac{dt}{dx} \end{aligned} \tag{3.8}$$

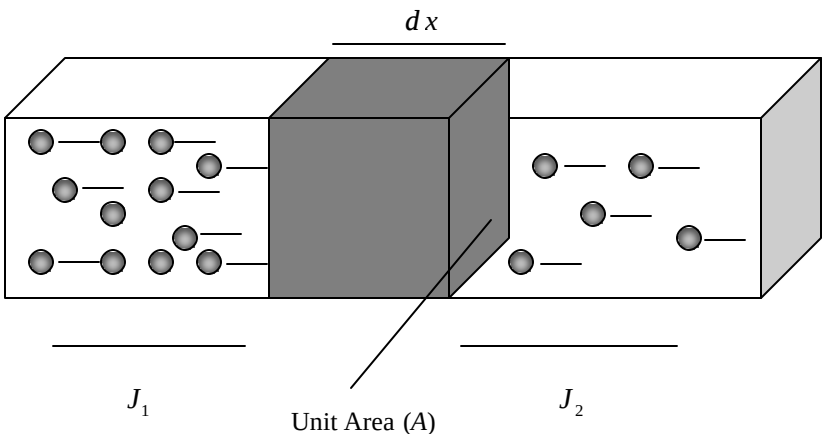

Figure 3.2: Representation of the flux through a unit area. The number of atoms that leave the thin volume is lower than the amount that enters the volume. The difference in the flux of the atoms entering the volume and the atoms leaving the volume is used to derive Fick's second law.

Further, the change in the concentration with time can be found by rearranging equation (3.8):

$$\frac{dC}{dt} = \left(J_1 - J_2\right)\frac{1}{dx}. \tag{3.9}$$

Since the width of the volume (dx) is very small (see Figure 3.2), the flux leaving the volume can be expressed as

$$J_2 = J_1 + \frac{\partial J}{\partial x}dx. \tag{3.10}$$

Inserting equation (3.10) into equation (3.9) leads to the continuity equation [67]

$$\frac{\partial C}{\partial t} = -\frac{\partial J}{\partial x}. \tag{3.11}$$

Substitution of Fick's first law (equation (3.5)) into equation (3.11) then gives

$$\frac{\partial C}{\partial t} = \frac{\partial}{\partial x}\left(D\frac{\partial C}{\partial x} \right), \tag{3.12}$$

and if variations in the concentration are ignored and D is assumed to be constant, equation (3.12) becomes [67]

$$\frac{\partial C}{\partial t} = D\frac{\partial^2 C}{\partial x^2}, \tag{3.13}$$

which is Fick's second law.

The next section focuses on the diffusion coefficient and random walks. It often provides more clarity to the meaning of the diffusion coefficient when a random walk approach is used.

3.3 Diffusion coefficient and random walks

The derivation of Fick's laws relied heavily on continuum diffusion equations. Sometimes it is also useful to describe diffusion in terms of the actual atomic motion. This is achieved by allowing one atom to perform a random walk in 2-dimensions or 3-dimensions. This particle is assumed to possess a mean value of the properties associated with the entire system being simulated [43].

For a particle performing a random walk in 2-dimensions, the individual step distance is assumed to be of equal length r. Any direction of motion has equal probability and the direction of motion is uncorrelated with the preceding jumps. A typical random walk performed by one particle is shown in Figure 3.3.

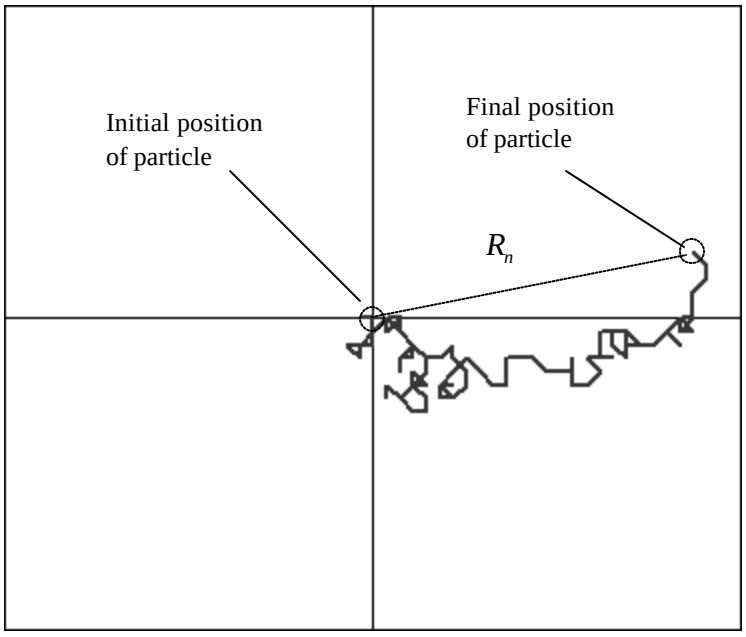

Figure 3.3: Illustration of a random walk performed by one particle

After performing n elementary jumps, the particle has moved an absolute distance $|R_n|$ from its origin. This distance can be written in vector form as follows:

$$\mathbf{R}_n = \sum_{i=1}^{n} \mathbf{r}_i \,, \tag{3.14}$$

where $\mathbf{r}_i$ are vectors representing the various jumps. Squaring both sides of equation (3.14) gives

$$\begin{aligned} R^2 = {} & \mathbf{r_1}\mathbf{r_1} + \mathbf{r_1}\mathbf{r}_2 + \ldots \mathbf{r_1}\mathbf{r}_n + \\ & \vdots \qquad\qquad\qquad\qquad \vdots \\ & + \mathbf{r}_n\mathbf{r_1} + \mathbf{r}_n\mathbf{r}_2 + \ldots \mathbf{r}_n\mathbf{r}_n \end{aligned} \tag{3.15}$$

which can be summarized by [43]

$$
\begin{aligned}
R_n^2 &= \sum_{i=1}^{n} \mathbf{r}_i \cdot \mathbf{r}_i + 2\sum_{i=1}^{n-1} \mathbf{r}_i \cdot \mathbf{r}_{i+1} + 2\sum_{i=1}^{n-2} \mathbf{r}_i \cdot \mathbf{r}_{i+2} + \cdots + 2\mathbf{r}_{n-1} \cdot \mathbf{r}_n \\
&= \sum_{i=1}^{n} r_i^2 + 2\sum_{j=1}^{n-1}\sum_{i=1}^{n-j} \mathbf{r}_i \cdot \mathbf{r}_{i+j} \\
&= nr^2 \left(1 + \frac{2}{n} \sum_{j=1}^{n-1}\sum_{i=1}^{n-j} \cos\Theta_{i,i+j} \right)
\end{aligned}
\tag{3.16}
$$

where $\Theta_{i,i+j}$ is the angle between the i^{th} and $(i+j)^{\text{th}}$ jump.

Since all jump directions are equally probable, the term containing the double sum is equal to zero as there are as many values of $-\Theta_{i,i+j}$ as $\Theta_{i,i+j}$. The most probable value of R_n therefore is zero and the most probable value of R_n^2 is given by

$$
\begin{aligned}
R_n^2 &= nr^2 \\
&= t\Gamma r^2 ,
\end{aligned}
\tag{3.17}
$$

where $n = t\Gamma$. When the random walk process is applied to three dimensions, exactly the same expression for R_n^2 is found [46].

According to Shewmon, et. al.[46], a relationship exists between the diffusion coefficient and the random walk process described above. This relationship is given by

$$
R_n^2 = t\Gamma r^2 = 6Dt , \tag{3.18}
$$

from which an expression for the diffusion coefficient is found:

$$
D = \frac{\Gamma r^2}{6} . \tag{3.19}
$$

Crystal Type	Correlation factor
2-dimensional square lattice	0.46694
2-dimensional hexagonal lattice	0.56006
Diamond	0.50000
Simple cubic	0.65311
Body-centred cubic	0.72722
Face-centred cubic	0.78146
Hexagonal close-packed	0.78121 (normal to c axis) 0.78146 (parallel to c axis)

Table 3.1: Correlation factors for self diffusion

This expression is the same as equation (3.6) derived in section 3.2.1.

At the beginning of this section it was mentioned that one of the assumptions made for this derivation is that there is no correlation between successive jumps. In real crystals this is not usually the case and jump probabilities do depend on the previous movements of the atom, where there is a certain chance that the atom can jump back to the original position. In order to compensate for correlation effects, equation (3.19) is multiplied by a constant *f*, also known as the correlation factor

$$D = \frac{\Gamma r^2}{6} f \ . \tag{3.20}$$

For random walk diffusion, the correlation factor is equal to unity. Several correlation factors for various crystal structures are listed in Table 3.1.

The correlation effect is most often found in vacancy diffusion, while interstitial diffusion is most often uncorrelated (valid only if the solution is dilute); therefore no correlation effects arise when the environment is symmetrical, as for a vacancy in a pure metal [43].

The relationship between the diffusion coefficient and temperature is derived in the next section.

3.4 Temperature dependence of D

The expression derived for the diffusion coefficient (equation (3.19)) is an elegant method of calculating the diffusion coefficient if the average jump frequency is known. However, calculating the jump frequency is not a simple task.

When an atom attempts a jump from one site to another, it encounters an energy (potential) barrier which it must overcome before it can jump, shown in Figure 3.4 This potential barrier arises from the strain inflicted by the diffusing atom on the lattice and the maximum strain energy is often referred to as the activation energy [45]. The work done to move an atom from one site to another is the same as the change in the Gibbs free energy for the local region, and the change in the Gibbs free energy is in turn equal to the maximum strain energy [46].

Suppose that the number of times an atom hits the potential barrier is Γ_0, which is the same as the oscillating frequency of the atom at its equilibrium position. There exists a certain probability (P_m) that the atom has enough energy at a particular time to overcome the potential barrier. This probability of motion is given by the Boltzman factor [45]

$$P_m = e^{\frac{-\Delta G_m}{RT}}, \tag{3.21}$$

where R is the universal gas constant, T is the temperature and ΔG_m is the change in the Gibbs free energy for migration given by [46]

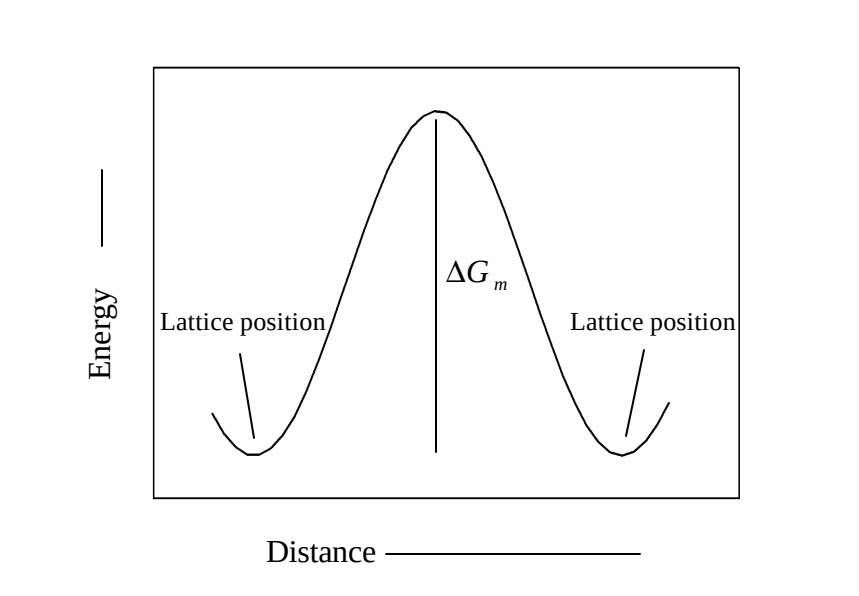

Figure 3.4: Graphical representation of the energy required for an atom to move from one lattice site to another.

$$\Delta G_m = \Delta H_m - T\Delta S_m, \tag{3.22}$$

with ΔH_m the enthalpy of migration and ΔS_m the entropy of migration.

Equation (3.21) can therefore be written as

$$P_m = \exp\frac{\Delta S_m}{R}\exp\frac{-\Delta H_m}{RT}. \tag{3.23}$$

It then follows that the average jump frequency for the diffusing atom is [45]

$$\begin{aligned}\Gamma &= \Gamma_0 P_m \\ &= \Gamma_0 e^{\frac{-\Delta G_m}{RT}}.\end{aligned} \tag{3.24}$$

If one assumes that the diffusing atom can only jump to neighbouring sites that are vacant, equation (3.24) must be multiplied by the probability that a vacancy exists via which the atom can move:

$$\Gamma = \Gamma_0 P_m P_v \tag{3.25}$$

where P_v is the probability that a vacancy exists at a lattice site and is equal to the mol fraction of vacancies, given by [39]

$$\begin{aligned} P_v &= X_v \\ &= \exp\frac{\Delta S_v}{R}\exp\frac{-\Delta H_v}{RT}, \end{aligned} \tag{3.26}$$

with ΔH_v the enthalpy of formation for one mole of vacancies and ΔS_v the excess entropy of one mole of vacancies. Physically ΔS_v is the result of the interaction between a vacancy and its nearest neighbours, while ΔH_v refers to the enthalpy required to take a vacancy from the surface of the crystal to a site within the crystal [39]. Equation (3.25) represents the average jump frequency in one dimension and it can easily be expanded to three dimensions by multiplying equation (3.25) by the number of nearest neighbour sites:

$$\Gamma = z\Gamma_0 P_m P_v \tag{3.27}$$

where z is the number of nearest neighbour sites.

Inserting equation (3.26) and (3.23) into equation (3.27) and grouping the temperature dependant and independent terms together leads to

$$\Gamma = z\Gamma_0 \exp\left(\frac{\Delta S_v + \Delta S_m}{R}\right)\exp\left(\frac{-\left(\Delta H_v + \Delta H_m\right)}{RT}\right) \tag{3.28}$$

A new expression for the diffusion coefficient is obtained by inserting equation (3.28) into equation (3.20):

$$\begin{aligned} D &= \frac{1}{6} zf\,\Gamma_0 P_m P_V r^2 \\ &= \frac{1}{6} zf\,\Gamma_0 r^2 \exp\left(\frac{\Delta S_v + \Delta S_m}{R}\right)\exp\left(\frac{-\left(\Delta H_v + \Delta H_m\right)}{RT}\right). \end{aligned} \tag{3.29}$$

Equation (3.29) can be rewritten with

$$D_0 = \frac{1}{6} zf\,\Gamma_0 r^2 \exp\left(\frac{\Delta S_v + \Delta S_m}{R}\right) \tag{3.30}$$

and

$$Q = \Delta H_v + \Delta H_m, \tag{3.31}$$

which in turn leads to the well known Arrhenius equation [38]

$$D = D_0 e^{\left(\frac{-Q}{RT}\right)}, \tag{3.32}$$

where Q is the activation energy and D_0 is a constant insensitive to temperature.

With equation (3.30) the constant D_0 can be calculated for simple-cubic, body-centred cubic and face-centred cubic crystal structures; the only factor that changes is the number

of nearest neighbour sites. For example, the constant D_0 for Copper diffusing in Copper (self diffusion) can be calculated by using the values listed in table 3.2.

Parameter	Value
$\Delta S_v + \Delta S_m \ \left(\text{J.mol}^{-1}.\text{K}^{-1}\right)$	$\approx 3R = 24.9$
$\Gamma_0 \ (\text{s}^{-1})$	$\approx 10^{12}$
$r \ \left(\overset{\text{o}}{\text{A}}\right)$ (lattice constant)	2.55
Correlation factor (FCC)	0.78146
Number of nearest neighbours	12

Table 3.2: Parameters used to calculate D_0 for copper [46].

$$
\begin{aligned}
D_0 &= \frac{1}{6} z f \Gamma_0 r^2 \exp\left(\frac{\Delta S_v + \Delta S_m}{R}\right) \\
&= \frac{1}{6} \times 12 \times 0.78146 \times 10^{12} \times \left(2.55 \times 10^{-10}\right)^2 \times \exp\left(\frac{24.9}{8.314}\right) \text{m}^2.\text{s}^{-1} \\
&= 2 \times 10^{-5} \text{m}^2.\text{s}^{-1}
\end{aligned}
$$

which is the same order of magnitude as the value $D_0 = 7.8 \times 10^{-5} \ \text{m}^2.\text{s}^{-1}$ given in Borg, et. Al. [43] as well as others [46].

It must be noted that the diffusion coefficient represented by equation (3.29) is applicable only to vacancy diffusion in that specific form. For interstitial diffusion, the terms ΔS_v and ΔH_v are equal to zero since this type of diffusion mechanism does not utilize substitutional vacancies to facilitate atomic motion. The mechanisms of diffusion mentioned in this section are now discussed in the next section, along with the ring mechanism of diffusion.

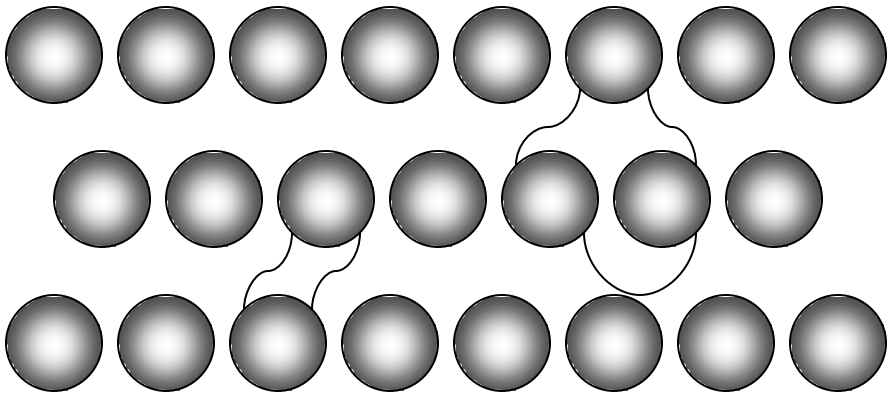

Figure 3.5: Graphical representation of ring diffusion.

3.5 Mechanisms of diffusion

The most important types of diffusion that take place in metals are interstitial, vacancy and ring diffusion. These types of diffusion influence the diffusion coefficient. The size of the atom and whether the diffusion is defect related also has an impact on the diffusion coefficient.

3.5.1 Ring diffusion

Figure 3.5 shows a ring diffusion process. Ring diffusion can only take place if the atoms are large enough to warrant a direct exchange rather than interstitial movement. The lattice will then undergo deformation and this deformation energy dictates the type of diffusion process that will take place. This distortion or deformation of the lattice is comparable to an interstitial mechanism for solvent atoms (this mechanism is discussed in section 3.5.3). The energy required to execute such a distortion is very high and therefore this type of mechanism is not very likely to take place [46]. If three or four atoms were to take part in the exchange, the distortion would be considerably less [39,46]. There is however very little evidence that this diffusion mechanism takes place [39].

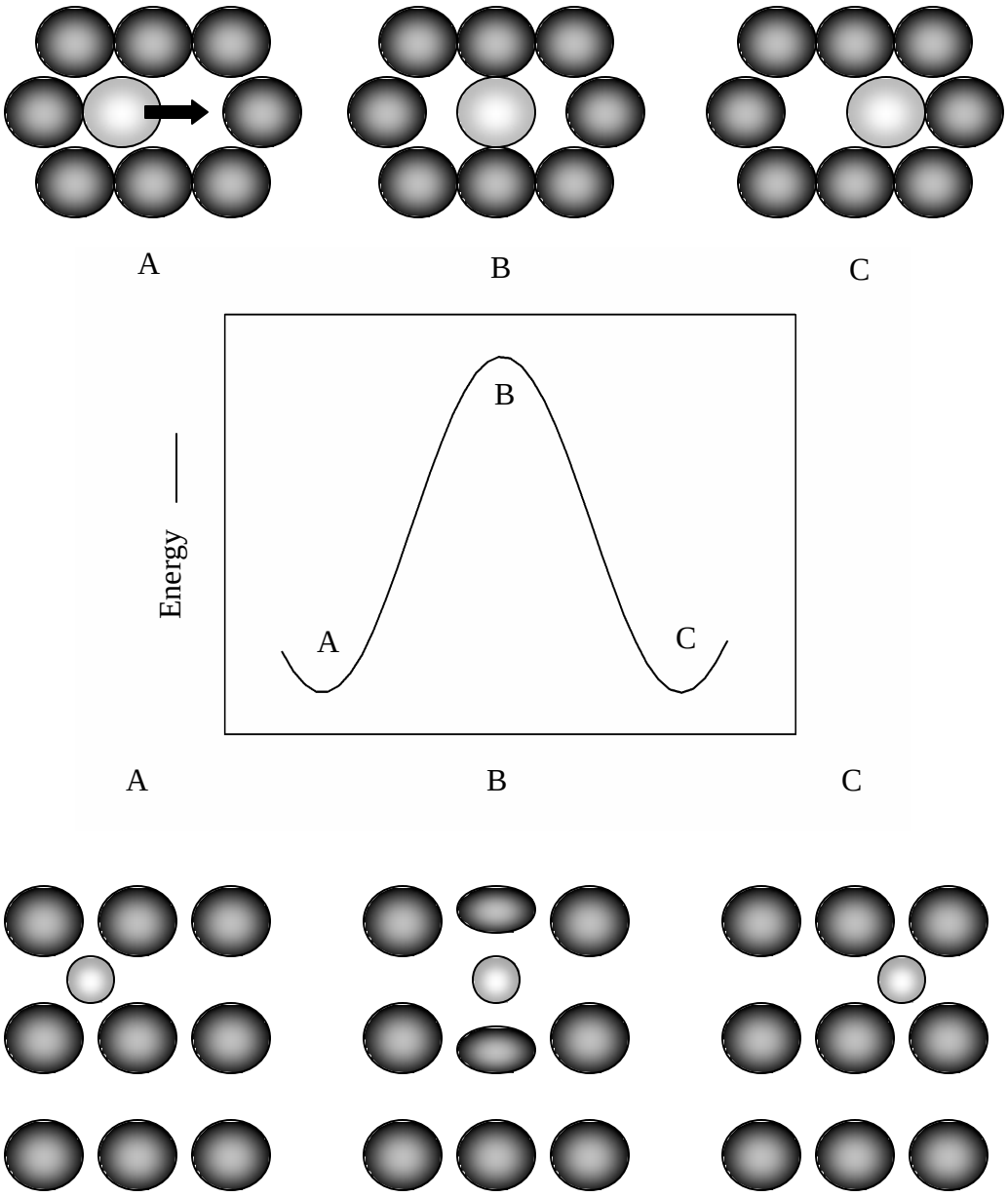

Figure 3.6: Graphical representation of vacancy and interstitial diffusion. The top graphic represents vacancy diffusion, while the bottom graphic represents interstitial diffusion. The potential barrier the diffusing atom encounters during the jump is shown in the middle figure. The energy required to move an interstitial atom is less than the energy required to move an atom through a vacancy mechanism.

3.5.2 Vacancy diffusion

This diffusion type depends on the availability of vacancies in the crystal lattice. Lattice vacancies occur in small equilibrium concentrations [45], but their contribution to the diffusion process is nevertheless important. For diffusion to take place, vacancies are required in the crystal lattice. The amount of vacancies in a lattice can be determined from [45]

$$N_v = N_0 e^{\left(\frac{-E_v}{RT}\right)}, \tag{3.33}$$

where N_0 represents the amount of lattice positions in the crystal and E_v is the vacancy formation energy. During vacancy diffusion the atoms in the crystal move via vacancies, as shown in Figure 3.6.

3.5.3 Interstitial diffusion

During this diffusion process, the diffusing atoms move interstitially, deforming the crystal as shown in Figure 3.6. This situation is very similar to vacancy diffusion. Interstitial diffusion is favoured by small atoms that do not deform the crystal significantly. The activation energy for interstitial diffusion is also less than that for vacancy diffusion, since there is no energy required to form vacancies (ΔH_v).

The following chapter introduces the reader to the principles of segregation as well as the differences between segregation and diffusion. Different methods of obtaining the surface segregation profiles are also discussed. This information is vital for the model presented in Chapter 5.

Chapter 4

Segregation Theory

4.1 Introduction

The movement of solute atoms from the bulk to the surface of a crystal, resulting in an increase of the surface concentration, is known as segregation. The movement of atoms during segregation is from an area with a low concentration (high energy) to an area with a high concentration (low energy) [2]. Segregation of atoms to the surface only takes place if the total Gibbs free energy of the crystal is lowered when the atoms move to the surface [69].

In this chapter, several models that describe segregation are discussed. A comparison between these models and the proposed Monte Carlo model is made in Chapter 6.

4.2 Segregation equilibrium

As mentioned above, segregation is defined as the movement of atoms from the bulk of a crystal to the surface of a crystal with the effect that the total energy of the crystal is

minimized. To avoid confusion, this definition is expanded further to include the following restrictions [2]:

1. The crystal is regarded as a closed system consisting of two phases, the surface and the bulk, which are both open systems (an open system is one where atoms can freely be exchanged between the two phases).
2. Atoms may be exchanged between the two phases until the total crystal energy is minimized.
3. The surface region is finite and the bulk is infinite.

For any closed system consisting of p phases, the equilibrium condition is given by [2,68]

$$\left(dU\right)_{S,V,n_i} = \sum_{n=1}^{p} dU^n \geq 0, \tag{4.1}$$

which means that the total energy U of the crystal is a minimum. Equation (4.1) can be expanded further [2]:

$$dU^n = T^n dS - P^n dV^n + dG^n \tag{4.2}$$

where T^n the temperature, S^n the entropy, P^n the pressure, V^n the volume of phase *?* and G^n the Gibbs free energy. If the temperature and pressure are the same for all the phases, equation (4.2) reduces to [2,3,48,64]

$$\left(dU\right)_{n_i} = \left(dG\right)_{n_i} \geq 0, \tag{4.3}$$

where dG is the change in the Gibbs free energy. Expanding the Gibbs free energy in terms of the chemical potential μ (the energy per atom or mol) leads to [2]:

$$G^n = \sum_{i=1}^{m} n_i^n \mu_i^n \,, \tag{4.4}$$

where n_i^n is the amount of mol of species i in phase *?* and μ_i^n is the chemical potential of species i in phase *?*. Also, for a system consisting of p phases, the total Gibbs free energy is given by

$$G_{Total} = \sum_{n=1}^{p} G^n = \sum_{n=1}^{p} \sum_{i=1}^{m} \left(n_i^n \mu_i^n \right). \tag{4.5}$$

It is now possible to calculate the change in the Gibbs free energy with equation (4.5) [2,69]:

$$dG = \sum_{n=1}^{p} \left[\sum_{i=1}^{m} \left(n_i^n d\mu_i^n \right) + \sum_{i=1}^{m} \left(d n_i^n \mu_i^n \right) \right]. \tag{4.6}$$

Comparing equation (4.6) with (4.3) leads to an expression for the equilibrium condition in terms of the chemical potential, which is

$$\sum_{n=1}^{p} \left[\sum_{i=1}^{m} \left(n_i^n d\mu_i^n \right) + \sum_{i=1}^{m} \left(d n_i^n \mu_i^n \right) \right] \geq 0 \,. \tag{4.7}$$

Equations (4.6) and (4.7) can be used to derive an expression for the equilibrium condition of atoms segregating from the bulk. This derivation is given in the next section.

4.2.1 Surface-Bulk equilibrium

In this section an equation is derived for the equilibrium condition for atoms that move from the bulk to the surface. The surface will be represented by (f) and the bulk by (B).

Further, it is assumed that the amount of atoms that can occupy the surface is finite and given by n^f, with $n^f = \text{constant}$. The bulk is infinite and the amount of atoms that can occupy this phase is also infinite. The atoms in the bulk are referred to as n^B. It is also assumed that atoms can move freely between the surface phase and the bulk phase.
For the system described above, equation (4.6) becomes [2,47,69]

$$dG = \left[\sum_{i=1}^{m}\left(n_i^f dm_i^f\right) + \sum_{i=1}^{m}\left(n_i^B dm_i^B\right)\right] + \left[\sum_{i=1}^{m}\left(dn_i^f m_i^f\right) + \sum_{i=1}^{m}\left(dn_i^B m_i^B\right)\right] \tag{4.8}$$

with n_i^f the amount of atoms of species i in the surface, m_i^f the chemical potential of species i in the surface, n_i^B the amount of atoms of species i in the bulk and m_i^B the chemical potential of species i in the bulk.

The first term in square brackets of equation (4.8) is the Gibbs-Duhem expression $\left(\sum_i n_i dm_i = 0\right)$ and is equal to zero [2,47] and equation (4.8) reduces to

$$dG = \sum_{i=1}^{m}\left(dn_i^f m_i^f\right) + \sum_{i=1}^{m}\left(dn_i^B m_i^B\right). \tag{4.9}$$

Since the amount of atoms in the surface layer is finite, the following holds true:

$$\sum_{i=1}^{m} n_i^f = n^f. \tag{4.10}$$

It can also be deduced that for every atom that jumps out of the surface and into the bulk another atom jumps into the surface from the bulk [2,69]. This is represented by equation (4.11):

$$dn_1^f + dn_2^f + ... + dn_m^f = 0. \tag{4.11}$$

Re-arranging equation (4.11) in terms of the preceding (m-1) terms leads to

$$-dn_m^f = dn_1^f + dn_2^f + ... + dn_{m-1}^f, \tag{4.12}$$

from which the change in Gibbs free energy is found by inserting equation (4.12) into equation (4.9):

$$\left[\sum_{i=1}^{m-1}\left(m_i^f - m_i^B - m_m^f + m_m^B\right)dn_i^f\right] \geq 0. \tag{4.13}$$

Equation (4.13) is only valid if [47,57]:

$$m_i^f - m_i^B - m_m^f + m_m^B = 0 \tag{4.14}$$

Equation (4.14) represents the equilibrium condition for atoms segregating from the bulk to the surface.

4.2.2 Equilibrium surface concentration

If one considers a binary alloy with the solvent matrix represented by a two $(m=2)$ and the solute represented by a one $(i=1)$, equation (4.14) becomes

$$m_1^f - m_1^B - m_2^f + m_2^B = 0. \tag{4.15}$$

According to Lupis, et. al. [68], the change in the chemical potential is given by

$$\Delta m_i = RT \ln a_i \tag{4.16}$$

where Δm_i is the difference between the chemical potential of i in a mixture compared to a pure state and a_i is called the activity coefficient. The activity coefficient of component i is defined by [2,68]

$$a_i = g_i X_i \tag{4.17}$$

where X_i is the concentration of element i and g_i is a constant. Substitution of equation (4.17) into equation (4.16) leads to

$$\Delta m_i = RT \ln a_i = RT \ln g_i X_i \tag{4.18}$$

or

$$m_i - m_i^0 = RT\left(\ln g_i + \ln X_i\right) \tag{4.19}$$

where m_i^0 represents the standard chemical potential of element i. If $g_i > 1$, it implies that the effective concentration of component i in the mixture is more than the physical concentration (X_i). If $g_i < 1$, it indicates that the effective concentration of component i in the mixture is less than the physical concentration (X_i). For an ideal solution, $g_i = 1$ [2,68] and equation (4.19) becomes [2]

$$m_i = m_i^0 + RT \ln X_i \tag{4.20}$$

which is the same as the regular solution model [2,68] when the interaction between the elements are ignored. Expanding equation (4.20) to include the interaction Ω_{ij} between the elements, the following two equations are found for a binary system [2,68]:

$$\begin{aligned} m_1^n &= m_1^{0,n} + \Omega_{12}\left(X_2^n\right)^2 + RT\ln\left(X_1^n\right) \\ m_2^n &= m_2^{0,n} + \Omega_{12}\left(X_1^n\right)^2 + RT\ln\left(X_2^n\right) \end{aligned} \tag{4.21}$$

where m_1^n represents the chemical potential of element 1 in phase n, $m_1^{0,n}$ represents the standard chemical potential of element 1 in phase n, m_2^n represents the chemical potential of element 2 in phase n, $m_2^{0,n}$ represents the standard chemical potential of element 2 in phase n, X_1 represents the concentration of element 1, X_2 represents the concentration of element 2 and Ω_{12} in the chemical interaction parameter between element 1 and 2.

In a binary alloy, there are two phases: the bulk and the surface. Equation (4.21) can then be expanded to four equations that include the different phases:

$$\begin{aligned} m_1^f &= m_1^{0,f} + \Omega_{12}\left(X_2^f\right)^2 + RT\ln\left(X_1^f\right) \\ m_2^f &= m_2^{0,f} + \Omega_{12}\left(X_1^f\right)^2 + RT\ln\left(X_2^f\right) \\ m_1^B &= m_1^{0,B} + \Omega_{12}\left(X_2^B\right)^2 + RT\ln\left(X_1^B\right) \\ m_2^B &= m_2^{0,B} + \Omega_{12}\left(X_1^B\right)^2 + RT\ln\left(X_2^B\right). \end{aligned} \tag{4.22}$$

By inserting equation (4.22) into equation (4.15) and rearranging, the Bragg-Williams equation is readily obtained [2,49,63,69]:

$$\frac{X_1^f}{1-X_1^f} = \frac{X_1^B}{1-X_1^B}\exp\left(\frac{\Delta G + 2\Omega_{12}\left(X_1^f - X_1^B\right)}{RT}\right) \tag{4.23}$$

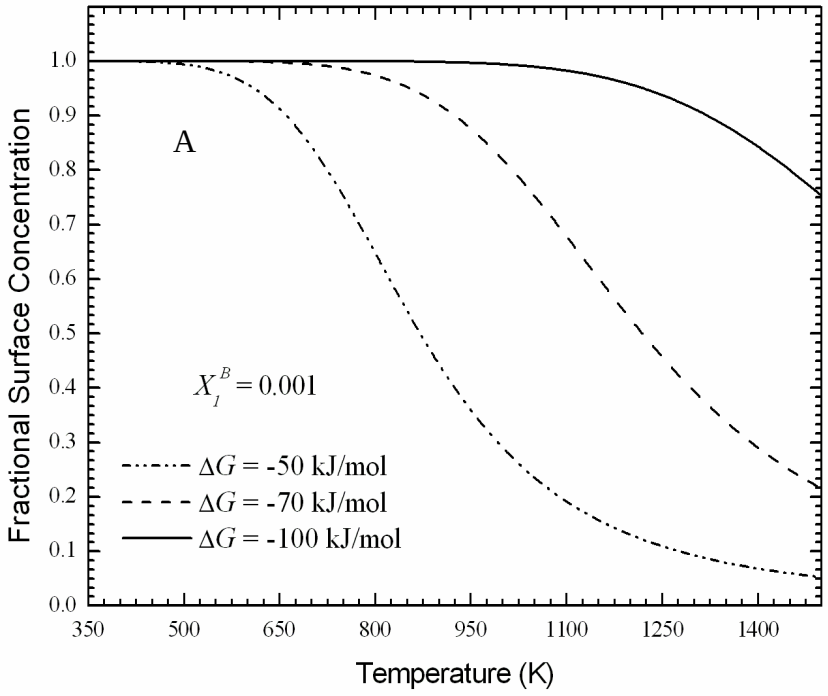

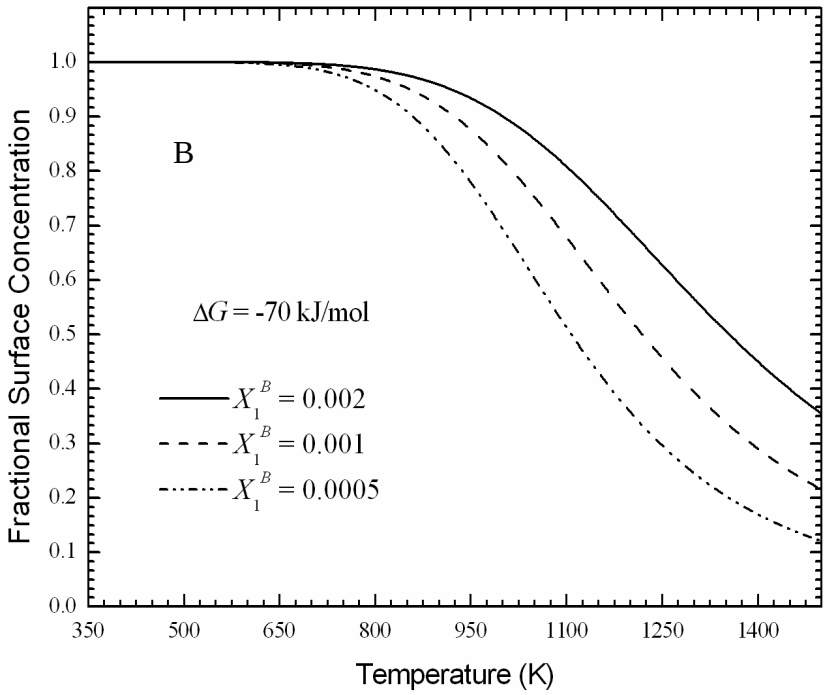

Figure 4.1: The depicted graphs show the equilibrium surface concentration as calculated with the Langmuir-McLean equation. In graph A, only the segregation energy is changed while in graph B, only the bulk concentration is changed.

with X_1^f the surface concentration of element 1, X_1^B the bulk concentration of element 1, $\Delta G = m_1^{0,B} - m_1^{0,f} - m_2^{0,B} + m_2^{0,f}$ the segregation energy and Ω_{12} the chemical interaction parameter between element 1 and 2.

For some conditions, the interaction parameter is zero, from which the Langmuir-McLean equation is found from equation (4.23) [2,48,50]:

$$\frac{X_1^f}{1-X_1^f} = \frac{X_1^B}{1-X_1^B}\exp\left(\frac{\Delta G}{RT}\right). \tag{4.24}$$

Examples of fractional surface concentration profiles generated by equation (4.24) are shown in Figure 4.1. In graph A, the bulk concentration, activation energy and the constant D_0 were held constant, with the only value adjusted being the segregation energy. If one considers for instance a surface coverage of 50 %, the influence of the segregation energy becomes clear: for a segregation energy of -50 kJ/mol, the surface is 50 % covered at a temperature of 870 K. If the segregation energy increases, the temperature at which 50 % coverage occurs also increases, e.g. at a segregation energy of -70 kJ/mol the surface is 50 % covered at a temperature of 1200 K. At higher temperatures, the atoms are more energetic and have enough energy to jump back into the bulk; at very high temperatures, the surface concentration is therefore lower.

When the segregation energy is held constant and the bulk concentration is adjusted, a different surface coverage is also observed, shown in graph B. In this case the surface concentration profiles shift towards higher temperatures with an increase in bulk concentration. Both the bulk concentration and the segregation energy therefore have a marked influence on the surface concentration of the segregating element.

The following two sections focus on the kinetics associated with surface segregation as well as the equilibrium conditions.

4.2.3 Infinite solution of Fick's equations

The purpose of this section is to provide a solution to Fick's first law, as it is often used to describe the kinetic part of segregation. The end product will be used in later stages as comparison for the segregation model described in Chapter 5.

Consider a crystal with a uniform bulk concentration. Suppose that the atoms segregating into the surface layer have no interaction with each other; therefore the rate of segregation is independent of the surface concentration.

There are two boundary conditions (shown in Figure 4.2) that are of importance in this derivation [65]:

$$C^x = 0 \qquad \text{for} \quad x = 0 \qquad \text{and} \quad t \geq 0,$$

and assuming that the bulk concentration of the segregating atoms is uniform,

$$C^x = C^B \qquad \text{for} \quad x > 0 \qquad \text{and} \quad t = 0.$$

Using the above boundary conditions to solve Fick's first law [2], it is possible to find an expression for the bulk concentration [2,65,69]:

$$C^x = C^B \operatorname{erf}\left(\frac{x}{2\sqrt{Dt}}\right) \tag{4.25}$$

where C^x represents the bulk concentration at position x after a time t, C^B represents the initial bulk concentration and D is the diffusion coefficient.

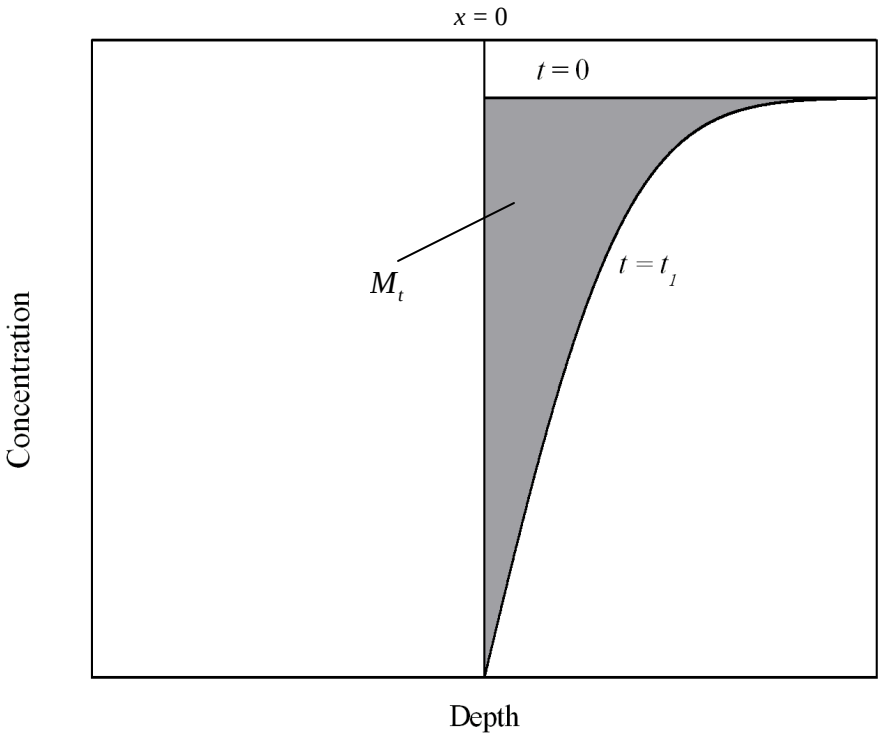

Figure 4.2: Boundary conditions used to solve Fick's first law.

Using equation (4.25), the flux can then be written as [65]

$$J_{x=0} = \left(D \frac{\partial C}{\partial x} \right)_{x=0} = \frac{DC^B}{\sqrt{p\,Dt}}. \tag{4.26}$$

It is possible to obtain the number of atoms (M_t) that pass through a surface A (at $x = 0$) in a given time t by integrating equation (4.26) [2,69]:

$$\begin{aligned} M_t &= A \int_{t=0}^{t} J dt \\ &= 2AC^B \left(\frac{Dt}{p} \right)^{\frac{1}{2}}. \end{aligned} \tag{4.27}$$

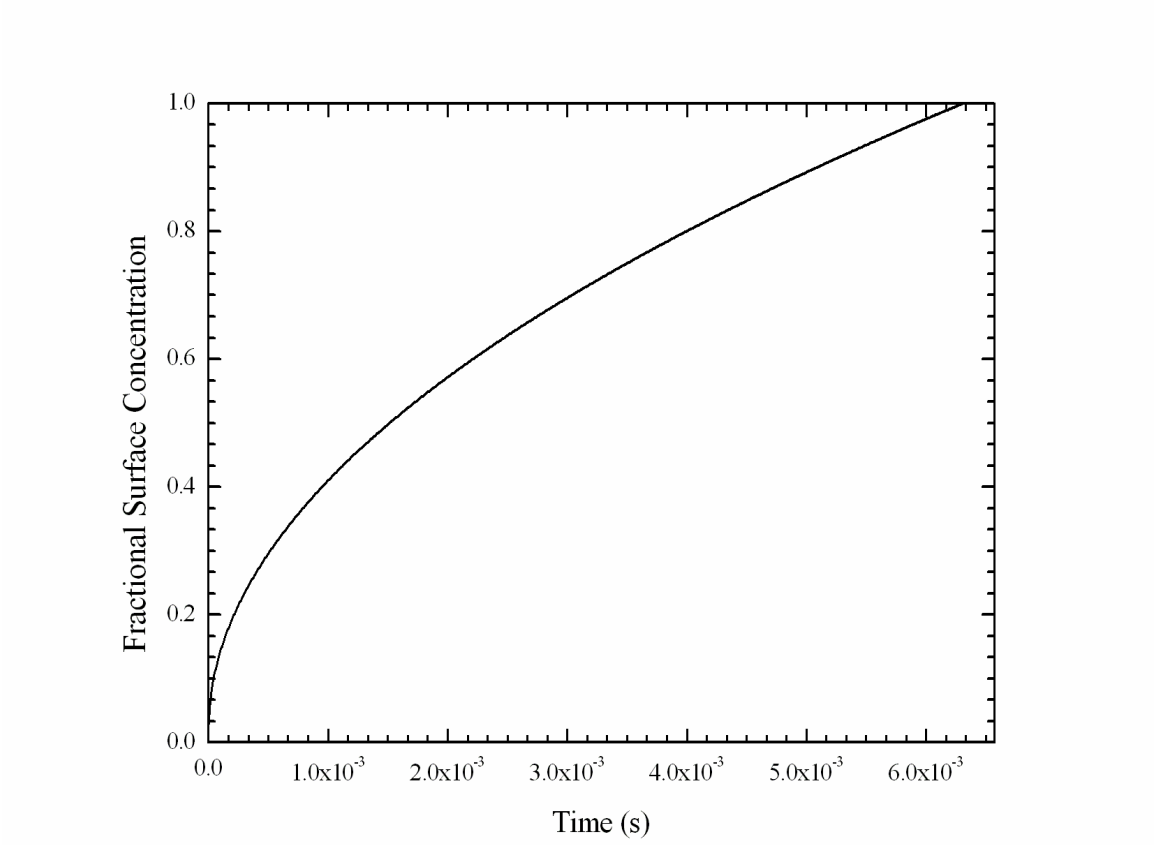

Figure 4.3: The change in the surface concentration with time is shown. The equilibrium surface concentration is not brought into consideration by this model.

The atoms moving through A is assumed to remain in the surface layer, the concentration of the segregating atoms in the surface can be determined by dividing equation (4.27) by the volume of the surface layer:

$$C^f = \frac{2AC^B\left(\frac{Dt}{p}\right)^{\frac{1}{2}}}{Ad} = \frac{2}{d}C^B\left(\frac{Dt}{p}\right)^{\frac{1}{2}}, \tag{4.28}$$

where d is the thickness of the layer, C^f is the surface concentration and C^B is the bulk concentration [69]. Since the initial concentration of the crystal is uniform, the

concentration of segregating elements in the surface layer is the same as the bulk concentration; the initial bulk concentration is therefore added to equation (4.28), which leads to [2,4,56-63,65,69]

$$C^f = C^B\left(1+\frac{2}{d}\left(\frac{Dt}{p}\right)^{\frac{1}{2}}\right). \tag{4.29}$$

Equation (4.29) is often used to calculate the surface concentration during segregation. Figure 4.3 shows a typical surface concentration profile generated with equation (4.29). From the conditions described at the beginning of this section, it is clear that this solution of Fick's first law predicts that the surface concentration will increase to infinity as time increases to infinity and therefore it cannot predict the equilibrium condition seen experimentally in surface segregation [48,51]. The next section describes the modified Darken model that describes both the kinetic and equilibrium conditions of a segregation curve.

4.2.3 The modified Darken model

The basic Darken model proposes that the flux of species i through a plane at $x = b$ is given by [2,49,69]

$$J_i = -M_i C_i^{(b)}\left(\frac{\partial m_i}{\partial x}\right)_{x=b} \tag{4.30}$$

where $C_i^{(b)}$ is the concentration of species i in the plane, m_i is the chemical potential of species i and M_i is the mobility of species i. The main difference between Fick's model described in the previous section and the Darken model is that the process that drives diffusion is different for the two. The Fick model assumes that the concentration gradient is the driving force while the Darken model assumes that the chemical potential gradient

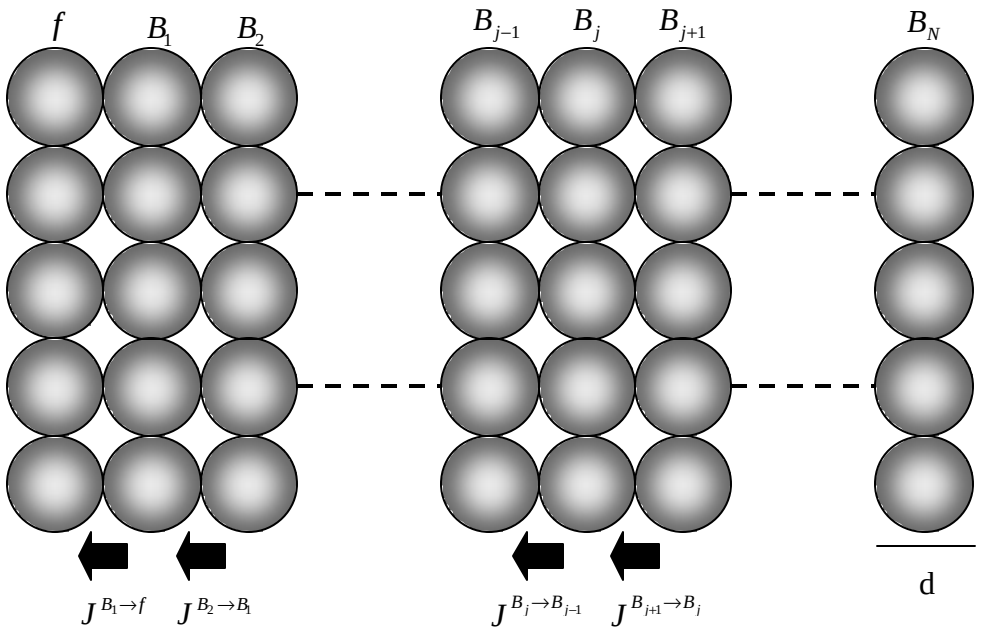

Figure 4.4: Representation of the atomic flux as proposed for the modified Darken model.

is the driving force behind diffusion. This means that the Darken model relies on the minimization of energy as the driving force behind diffusion.

The modified Darken model proposed by Du Plessis [2,47] defines a crystal as a system of discrete layers parallel to the surface layer, as shown in Figure 4.4. Du Plessis also rewrote the term $\frac{\partial m_i}{\partial x}$ in a discrete form:

$$-\frac{\partial m_i}{\partial x} = \frac{\Delta m_i^{(j+1\to j)}}{d} \tag{4.31}$$

with d the thickness of the layers. The change in the chemical potential was also rewritten as (the derivation is given in Chapter 5, equations (5.1)-(5.13))

$$\Delta m_i^{(j+1\to j)} = \left(m_i^{(j+1)} - m_i^{(j)}\right) - \left(m_m^{(j+1)} - m_m^{(j)}\right), \tag{4.32}$$

where $m_i^{(j+1)}$ is the chemical potential of species i in layer j+1, $m_i^{(j)}$ is the chemical potential of species i in layer (j), $m_m^{(j+1)}$ is the chemical potential of species m in layer j+1 and $m_m^{(j)}$ is the chemical potential of species m in layer j.

If atoms move from layer j+1 to layer j, the flux of atoms (equation (4.30)) can be written as [2,47,69]

$$J_i^{(j+1\to j)} = -M_i C_i^{(j+1)} \frac{\Delta m_i^{(j+1\to j)}}{d}. \tag{4.33}$$

A similar equation can be obtained for atoms moving from layer j to j+1:

$$J_i^{(j\to j+1)} = -M_i C_i^{(j)} \frac{\Delta m_i^{(j+1\to j)}}{d}. \tag{4.34}$$

Since the minimization of the Gibbs free energy is the driving force behind segregation, the change in the chemical potential will determine which one of equations (4.33) or (4.34) is used in calculating the flux $J_i^{(j\to j+1)}$. If $\Delta m_i^{(j+1\to j)} > 0$, the Gibbs free energy will decrease when atoms move from layer j+1 to j, and equation (4.33) is used in the calculations. If $\Delta m_i^{(j+1\to j)} < 0$, the Gibbs free energy will decrease when atoms move from layer j to j+1, and equation (4.34) is used in the calculations.

The rate at which the concentration in layer j is changing can be calculated with equations (4.33) and (4.34) [2,69]:

$$\frac{\partial C_i^{(j)}}{\partial t} = \frac{\left(J_i^{(j+1\to j)} - J_i^{(j\to j-1)}\right)}{d}. \tag{4.35}$$

Expanding equation (4.35) in terms of a system of $(m-1)(N+1)$ equations enables the calculation of the rate at which species i's concentration increases in layer j [69]:

$$
\begin{aligned}
\frac{\partial X_i^{(f)}}{\partial t} &= \left(\frac{M_i^{(B_1 \to f)} X_i^{(B_1)}}{d^2} \Delta m_i^{(B_1 \to f)} \right) \\
\frac{\partial X_i^{(B_1)}}{\partial t} &= \left(\frac{M_i^{(B)} X_i^{(B_2)}}{d^2} \Delta m_i^{(B_2 \to B_1)} - \frac{M_i^{(B_1 \to f)} X_i^{(B_1)}}{d^2} \Delta m_i^{(B_1 \to f)} \right) \\
&\vdots \\
\frac{\partial X_i^{(j)}}{\partial t} &= \left(\frac{M_i^{(B)} X_i^{(j+1)}}{d^2} \Delta m_i^{(j+1 \to j)} - \frac{M_i^{(B)} X_i^{(j)}}{d^2} \Delta m_i^{(j \to j-1)} \right). \\
&\vdots
\end{aligned}
\tag{4.36}
$$

The system of differential equations can be solved numerically, enabling the calculation of the concentration of species *i* in any layer as a function of time. In studies involving ideal binary alloys, the above rate equations are often rewritten with the aid of equations (4.22) and (4.14) to allow binary alloy specific calculations:

$$
\begin{aligned}
\frac{\partial X_1^{(f)}}{\partial t} &= \left(\frac{M_1^{(B_1 \to f)} X_1^{(B_1)}}{d^2} \right) \left[\Delta G + RT \ln \left(\frac{X_1^{(B_1)} X_2^{(f)}}{X_1^{(f)} X_2^{(B_1)}} \right) \right] \\
\frac{\partial X_1^{(B_1)}}{\partial t} &= \left(\frac{M_1^{(B)} X_1^{(B_2)}}{d^2} \right) \left[RT \ln \left(\frac{X_1^{(B_2)} X_2^{(B_1)}}{X_1^{(B_1)} X_2^{(B_2)}} \right) - RT \ln \left(\frac{X_1^{(B_1)} X_2^{(f)}}{X_1^{(f)} X_2^{(B_1)}} \right) \right] \\
&\vdots \\
\frac{\partial X_1^{(B_j)}}{\partial t} &= \left(\frac{M_1^{(B)} X_1^{(B_{j+1})}}{d^2} \right) \left[RT \ln \left(\frac{X_1^{(B_{j+1})} X_2^{(B_j)}}{X_1^{(B_j)} X_2^{(B_{j+1})}} \right) - RT \ln \left(\frac{X_1^{(B_j)} X_2^{(B_{j-1})}}{X_1^{(B_{j-1})} X_2^{(B_j)}} \right) \right]. \\
&\vdots
\end{aligned}
\tag{4.37}
$$

The above rate equations is capable of simulating both the kinetic and equilibrium conditions associated with segregation, as indicated in Figure 4.5.

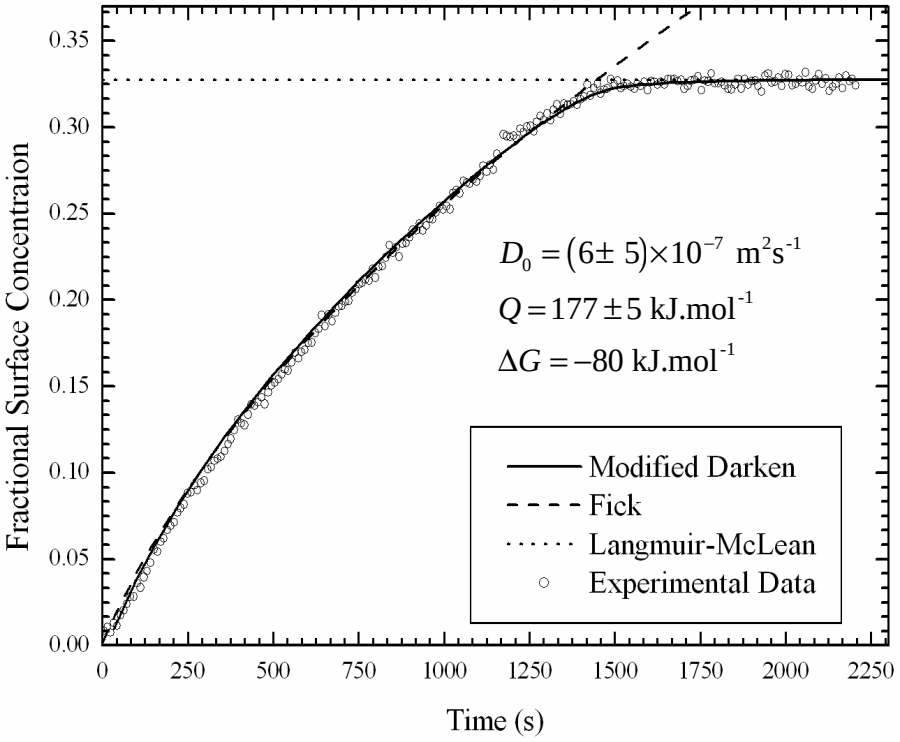

Figure 4.5: The figure shows a comparison of the surface segregation as calculated with Fick's model and the modified Darken model. The kinetic part of segregation is similar for both models. Fick's model is unable to describe the equilibrium surface concentration, while the modified Darken follows the experimental data closely [48].

An experimental segregation study was conducted by Erasmus, et. al. [48]. This study focused on the segregation of Sb from Cu crystals and a typical result from the study is shown in Figure 4.5. The dashed line represents the theoretical fit obtained from Fick's model. The Fick model accurately describes the kinetics of segregation from time $t = 0$ s to time $t = 1100$ s. However, the model cannot describe the equilibrium condition seen from the experimental data and predicted by the Langmuir-McLean equation (dotted line).

The solid line in Figure 4.5 is the theoretical fit of the experimental data obtained from the modified Darken model. This model accurately describes both the kinetic and equilibrium conditions associated with segregation and the equilibrium value obtained

from the fit also matches the value predicted by the Langmuir-McLean equation. Since the modified Darken model correctly describes the segregation phenomenon, it will be used as the basis of the Monte Carlo model presented in the next chapter.

Chapter 5

Monte Carlo model of segregation

5.1 Introduction

The theoretical model described in this chapter is a variation of the modified Darken model described in Chapter 4: the change in chemical potential is again used to determine the atomic motion.

In 1989 Du Plessis, et. al. [57] published a derivation for the space derivative of the chemical potential. Parts of this derivation are similar to the derivation discussed in the segregation equilibrium section of Chapter 4. Even though there are similarities, the derivation forms an important part of the model discussed in this chapter. The following section is an excerpt of the published derivation.

Surface segregation is a discrete phenomenon and therefore the discrete model forms the basis of the derivation and the conclusions presented in the next section [2,47].

5.1.1 The change in the chemical potential

Consider a crystal divided into N+1 layers. The change in the Gibbs free energy can be calculated when atoms of species i move from layer j+1 to layer j. The Gibbs free energy

of the two layers involved, j+1 and j, consisting of an alloy containing m different components is given by [57,68]

$$G = \sum_{i}^{m} n_i^{(j)} m_i^{(j)} + \sum_{i}^{m} n_i^{(j+1)} m_i^{(j+1)} \tag{5.1}$$

where $n_i^{(j)}$ is the number of moles of species i in the j-th layer, $m_i^{(j)}$ is the chemical potential of species i in the j-th layer, etc.

From equation (5.1), it is clear that the variation in the Gibbs free energy is equal to [57]

$$dG = \sum_{i}^{m} \left(d n_i^{(j)} m_i^{(j)} + n_i^{(j)} dm_i^{(j)} \right) + \sum_{i}^{m} \left(d n_i^{(j+1)} m_i^{(j+1)} + n_i^{(j+1)} dm_i^{(j+1)} \right). \tag{5.2}$$

Applying the Gibbs-Duhem relation $\left(\sum_i n_i dm_i = 0 \right)$ to equation (5.2) it follows that [2,57]

$$dG = \sum_{i}^{m} \left(d n_i^{(j)} m_i^{(j)} + d n_i^{(j+1)} m_i^{(j+1)} \right). \tag{5.3}$$

If the atomic flux is from layer j+1 to j, it follows that

$$d n_i^{(j)} = -d n_i^{(j+1)} \tag{5.4}$$

and by substituting this into equation (5.3), it becomes

$$dG = \sum_{i}^{m} d n_i^{(j)} \left(m_i^{(j)} - m_i^{(j+1)} \right). \tag{5.5}$$

For substitutional alloys, the total number of moles (n) in a layer (j) is fixed [2,57]. This leads to the following relations:

$$\sum_{i}^{m} n_i^{(j)} = n \tag{5.6}$$

and

$$\sum_{i}^{m} d n_i^{(j)} = 0 \,. \tag{5.7}$$

From equation (5.7), it follows that the $d n_i^{(j)}$ terms are not independent and by writing the m-th term ($d n_m^{(j)}$) in terms of the previous (m-1) terms (equation (5.8)), the (m-1) terms ($d n_i^{(j)}$) are now independent [2,57].

$$d n_m^{(j)} = -\sum_{i}^{m-1} d n_i^{(j)} \tag{5.8}$$

Rearranging equation (5.5) leads to

$$dG = \sum_{i}^{m-1} d n_i^{(j)} \left(m_i^{(j)} - m_i^{(j+1)} \right) + d n_m^{(j)} \left(m_m^{(j)} - m_m^{(j+1)} \right) \tag{5.9}$$

Inserting equation (5.8) into equation (5.9), it is found that [48,57,68]

$$dG = -d n_i^{(j)} \left(m_i^{(j)} - m_i^{(j+1)} - m_m^{(j)} + m_m^{(j+1)} \right); \tag{5.10}$$

now by rearranging equation (5.10) it leads to

$$\frac{dG}{d n_i^{(j)}} = -\left(m_i^{(j)} - m_i^{(j+1)} - m_m^{(j)} + m_m^{(j+1)} \right) \tag{5.11}$$

which may be written as

$$\frac{dG}{dn_i^{(j)}} = -\Delta m_i . \tag{5.12}$$

The term $\frac{dG}{dn_i^{(j)}}$ is the change in the Gibbs free energy per mol [57,68], which is the definition for the change in chemical potential; therefore equation (5.11) can be written as [57,68]:

$$\Delta m_i^{(j \to j+1)} = \left(m_i^{(j)} - m_i^{(j+1)} - m_m^{(j)} + m_m^{(j+1)} \right). \tag{5.13}$$

With this equation, the change in the chemical potential (energy) of a crystal can be calculated when atoms of species *i* move from layer *j* to layer *j*+1. The CPMC model presented in this chapter utilizes equation (5.13) to determine whether the attempted atomic jump will *increase* or *decrease* the total energy of the crystal. Only jumps that lower the crystal energy are allowed.

5.1.2 The change in the chemical potential for bulk motion

For a crystal divided into *N*+1 layers, parallel to the surface, an atom in the bulk can move either from layer *j* to *j*-1 or from layer *j* to *j*+1, depending on which move results in the crystal energy being lowered. This section describes the method used to determine the change in the chemical potential if all three the atomic layers involved are bulk layers. The following equation gives the chemical potential for element 1 dissolved in a bulk layer of a binary crystal [2,48,59,69]:

$$m_1^{(j)} = m_1^{0,(j)} + \Omega_{12}(1 - X_1^{(j)})^2 + RT \ln X_1^{(j)} \tag{5.14}$$

where $m_1^{(j)}$ is the chemical potential for element 1 in the bulk layer j, $m_1^{0,(j)}$ is the standard chemical potential for element 1 in the bulk, O_{12} is the interaction parameter between elements 1 and 2, $X_1^{(j)}$ is the concentration of element 1 in layer j, R is the universal gas constant and T is the temperature. Equation (5.14) can now be rewritten in the following form:

$$m_1^{(j)} = m_1^{0,(j)} + m_1'^{(j)} \tag{5.15}$$

with

$$m_1'^{(j)} = \Omega_{12}(1 - X_1^{(j)})^2 + RT \ln X_1^{(j)}. \tag{5.16}$$

By inserting equation (5.15) into equation (5.13), it follows that

$$\begin{aligned}\Delta m_1^{(j\to j+1)} = &\left[\left(m_1'^{(j)} - m_1'^{(j+1)}\right) - \left(m_2'^{(j)} - m_2'^{(j+1)}\right)\right] \\ &+ \left[\left(m_1^{0,(j)} - m_1^{0,(j+1)}\right) - \left(m_2^{0,(j)} - m_2^{0,(j+1)}\right)\right]\end{aligned} \tag{5.17}$$

Since the standard chemical potential of an element is the same in both bulk layers (j and j+1) [2,47,69], it is clear that the second square bracket is equal to zero and therefore equation (5.17) simplifies to

$$\Delta m_1^{(j\to j+1)} = \left(m_1'^{(j)} - m_1'^{(j+1)}\right) - \left(m_2'^{(j)} - m_2'^{(j+1)}\right). \tag{5.18}$$

A similar equation for movements from layer j to j-1 can be obtained by following the same procedure as shown above:

$$\Delta m_1^{(j\to j-1)} = \left(m_1'^{(j)} - m_1'^{(j-1)}\right) - \left(m_2'^{(j)} - m_2'^{(j-1)}\right). \tag{5.19}$$

The Chemical Potential Monte Carlo model extensively utilizes equations (5.18) and (5.19) to determine whether the attempted move of an atom will *increase* or *decrease* the total energy of the crystal. Only moves that *decrease* the energy are acceptable.

5.1.3 The change in the chemical potential for bulk to surface and surface to bulk motion

The standard chemical potential for an atom in a surface layer is different from an atom in a bulk layer; therefore, the second square bracket in equation (5.17) is not zero. This difference in the standard chemical potentials is the segregation energy (ΔG) and therefore equation (5.17) simplifies to [52,68]

$$\Delta m_1^{(f\to B_1)} = \left[\left(m_1'^{(f)} - m_1'^{(B_1)}\right) - \left(m_2'^{(f)} - m_2'^{(B_1)}\right)\right] + \Delta G_1^{f\to B_1} \tag{5.20}$$

with

$$\Delta G_1^{f\to B_1} = \left(m_1^{0,(f)} - m_1^{0,(B_1)}\right) - \left(m_2^{0,(f)} - m_2^{0,(B_1)}\right). \tag{5.21}$$

In equation (5.20) and (5.21), the surface layer is represented by f and the first bulk layer is represented by B_1. The same procedure as above lead to similar equations for atoms moving from the surface layer into the bulk [52,68]:

$$\Delta m_1^{(B_1\to f)} = \left(m_1'^{(B_1)} - m_1'^{(f)}\right) - \left(m_2'^{(B_1)} - m_2'^{(f)}\right) + \Delta G_1^{B_1\to f} \tag{5.22}$$

with

$$\begin{aligned}\Delta G_1^{B_1\to f} &= \left(m_1^{0,(B_1)} - m_1^{0,(f)}\right) - \left(m_2^{0,(B_1)} - m_2^{0,(f)}\right)\\ &= -\Delta G_1^{f\to B_1}\end{aligned}. \tag{5.23}$$

The segregation energy is responsible for the enrichment of the surface layer by the segregating element. Similar equations can be derived for element 2.

5.2 The Chemical Potential Monte Carlo (CPMC) model

This section describes a Monte Carlo model that uses chemical potential calculations to simulate bulk-to-surface segregation as well as diffusion in uniform and multilayered samples. The calculation routine is initiated with the selection of a random atom inside a crystal matrix. The change in chemical potential derived in the previous sections then determines the direction of motion available to the selected atom.

5.2.1 Bulk to bulk movements

For a bulk atom, equations (5.18) and (5.19) are used to determine the direction of atomic motion. If $\Delta m_1^{(j\to j+1)} > 0$, the total energy of the crystal will be decreased by moving the selected atom from layer j to layer j+1. The same applies if $\Delta m_1^{(j\to j-1)} > 0$, where the total energy of the crystal will be decreased by moving the selected atom from layer j to layer j-1. If both $\Delta m_1^{(j\to j+1)}$ and $\Delta m_1^{(j\to j-1)} > 0$, the direction of the atomic jump is determined by the largest change in the chemical potential. Therefore if $\Delta m_1^{(j\to j-1)} < \Delta m_1^{(j\to j+1)}$, the selected atom is moved from layer j to layer j+1. If $\Delta m_1^{(j\to j-1)} > \Delta m_1^{(j\to j+1)}$, the selected atom is moved from layer j to layer j-1. All the possible moves that the selected atom can execute are shown in Figure 5.1: the neighbouring atoms are marked from 1 to 8.

If the atom should move from layer j to j+1, the possible moves are limited to three (2,3 or 4), as shown in Figure 5.1. A random number (N_R) is chosen in the interval $2 \le N_R \le 4$, with N_R an integer, which determines the direction the randomly selected

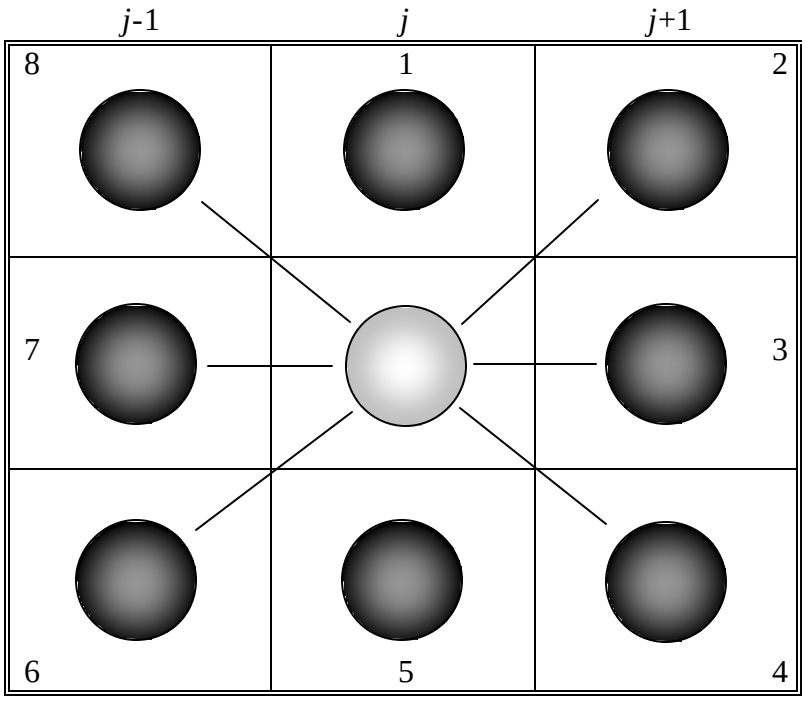

Figure 5.1: Schematic representation of all possible directions of motion for a randomly selected atom. The neighbouring atoms are numbered clockwise around the randomly selected atom. The directions of motion described in section 5.2.1 are equivalent for an exchange between the selected (center) atom and a neighbouring atom by selecting a random number which corresponds to the direction of motion.

atom will move. This random number corresponds to an exchange with an atom of the same number.

If the exchanging atoms are of the same type, as represented by Figure 5.2 (move 3), a new random number determines the direction of motion.

In this case, the randomly selected atom can only be exchanged with atom 2 or 4. If two atoms in the layer adjacent to the selected atom are the same type of atoms as the selected atom, only one direction of movement is possible.

If the change in chemical potential indicates that the randomly selected atom must move to layer j+1, but all the atomic positions in layer j+1 are occupied by atoms that are the same type as the chosen atom, the change in chemical potential for a move to the left

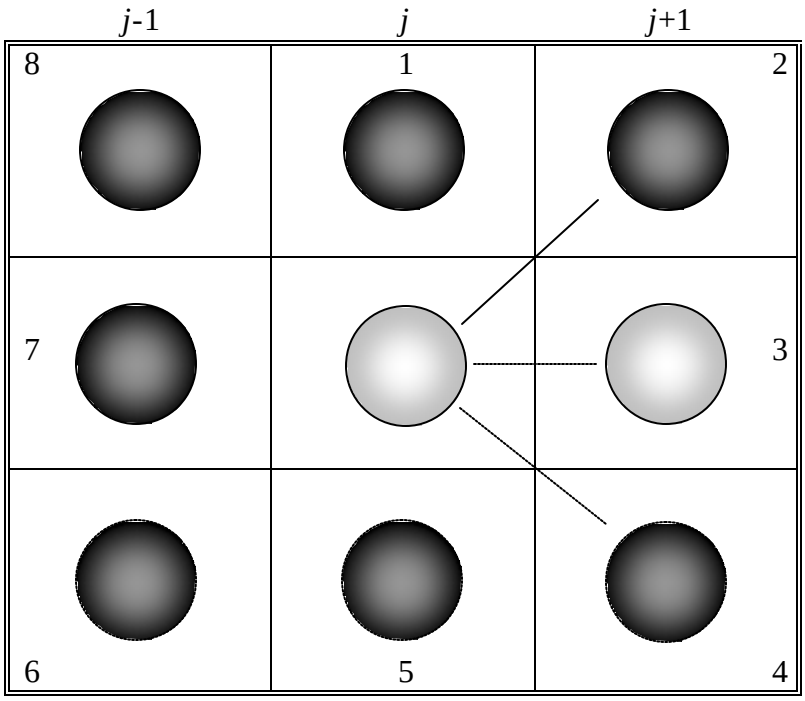

Figure 5.2: Special situation of atomic motion from layer j to j+1. Only 2 directions of motion exist: an exchange with either atom 2 or 4.

determines the action taken by the program. An atomic jump is only allowed if $\Delta m_1^{(j \to j-1)} > 0$, resulting in a decrease in crystal energy.

For movements from layer j to layer j-1, equation (5.19) comes into play. If $\Delta m_1^{(j \to j-1)} > 0$, moving the selected atom from layer j to layer j-1 decreases the energy of the crystal.

In the case of movement to layer j-1, a random number (integer) is again generated, but in this instance, the interval is $6 \le N_R \le 8$ (see Figure 5.1). The conditions of atomic motion described for an atomic jump from layer j to j+1 are again implemented for the jump described above.

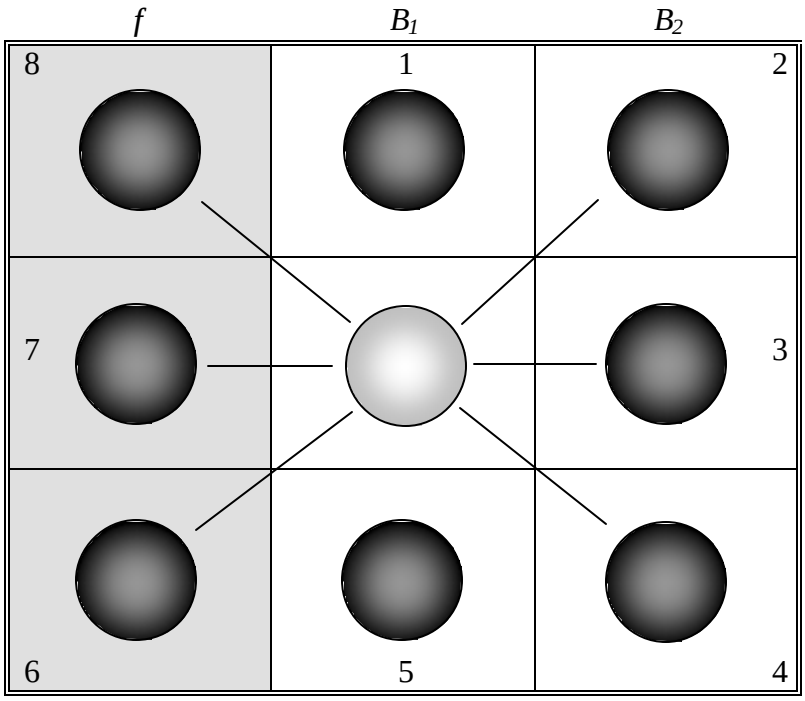

Figure 5.3: Schematic representation atomic motion involving the surface layer. The greyed out layer represents the surface layer. The directions of motion described in section 5.2.2 are equivalent for an exchange between the selected (center) atom and a neighbouring atom by selecting a random number which corresponds to the direction of motion. Atoms 6, 7 and 8 are surface atoms, with the atomic motion of these atoms influenced by the segregation energy associated with the surface layer.

5.2.2 Bulk to surface and surface to bulk movements

For motion in the surface layer or the first bulk layer, two situations can be identified: the randomly selected atom lies in the surface layer or the randomly selected atom lies in the first bulk layer. Figure 5.3 represents the latter of the two foregoing cases. If the energy characteristics of the surface layer (f) differs from the first bulk layer (B_1), segregation of atoms into the surface layer can occur. Atoms in the surface layer can move into the bulk, but the segregation energy ($\Delta G_1^{f \to B}$) reduces the rate of surface to bulk jumps for species 1, resulting in a higher surface concentration of species 1.

Equation (5.20) governs motion from the surface to the first bulk layer, and equation (5.22) governs motion from the first bulk layer to the surface. The conditions described

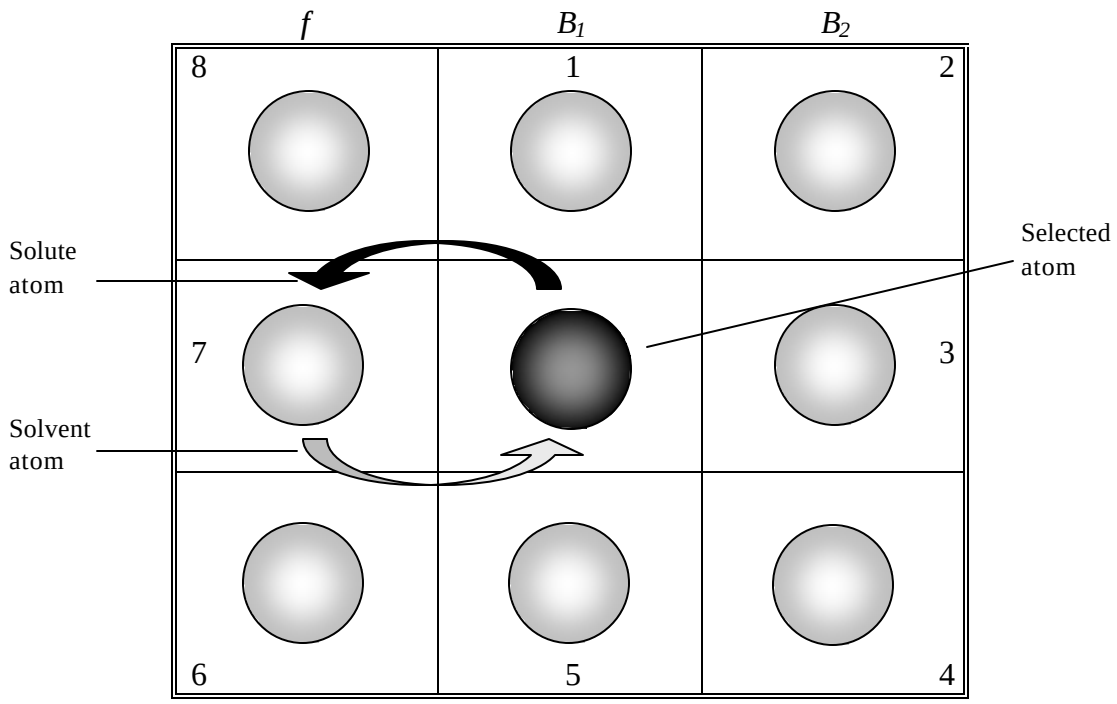

Figure 5.4: Representation of atomic motion if the randomly selected atom is a solvent atom instead of a solute atom. The motion is the reverse of the motion for solute atom.

in section 5.1.3 direct atomic motion in the surface/first bulk layer. For an atom in the surface, calculations involving layer j-1 are ignored, since the surface layer is the final layer in the crystal.

If a bulk atom is randomly chosen, the change in chemical potential associated with the solute element still controls the atomic jumps. The conditions for atomic motion described above remain the same for both solute and solvent atoms; however, the direction of atomic motion is the reverse of jumps involving solute atoms, i.e. atoms jump *into* layer j instead of *out* of layer j as shown in Figure 5.4.

5.3 Atomic motion and the diffusion coefficient

Before an atomic jump is executed, the diffusion coefficient for each element is calculated with the following equation [38]:

$$D_i = D_{i,0} e^{\frac{-Q_i}{RT}}, \tag{5.24}$$

where $D_{i,0}$ is the standard diffusion coefficient for element i, Q_i is the activation energy of element i, R is the universal gas constant and T is the temperature. To emulate the influence of the diffusion coefficients on the diffusion rate of the two elements, the following fraction is employed:

$$f_i = \frac{D_i}{\sum_{i=1}^{m} D_i}. \tag{5.25}$$

This fraction (f_i) limits the number of jumps a particular species i can perform. For example, if both diffusion coefficients are the same, equation (5.25) yields a fraction of 0.5. This means that both species have equal probability of performing a jump. If the fraction is e.g. $\frac{1}{3}$, i.e. $D_2 = 2D_1$, only a third of the jumps allowed will be species 1 and two thirds of the jumps will be species 2.

The accuracy of the CPMC model was studied by using various activation energies, D_0 values and segregation energies. These profiles were then compared to the modified Darken model as well as the Fick's model. The results of the comparison are given in the next chapter.

Chapter 6

Results and discussion

6.1 Introduction

The surface segregation profiles generated with the CPMC model are discussed in this chapter. A total of eight different calculations were performed for various segregation and diffusion parameters applied to a crystal with a uniform atomic concentration. The profiles generated were compared to profiles obtained from the modified Darken model and Fick's model described in Chapter 4. The purpose of the comparisons is to investigate whether a similar trend is observable between the CPMC model and the existing models. Parallel computations with the CPMC model were also investigated and the profiles generated by parallel computation were compared to a profile generated on a single computer.

6.2 Calculations

To determine the accuracy and validity of the CPMC model, simulations were performed for different values of the diffusion coefficient D_o, activation energy Q and segregation energy ΔG. The crystal had a height of 2000 atoms and a width (bulk depth) of 300

atoms (2000×300), with a uniform atomic concentration of 2 at%. The choice of the crystal width was made specifically to retain a certain level of accuracy and to minimize boundary effects [2]. This value for the crystal width is determined from the concentration of the dissolved atoms in the crystal. Suppose that the maximum surface concentration is 100 % and that the bulk concentration is 5 %. Ideally, atoms from the first twenty layers must move into the surface to completely occupy the surface layer. In practice there is diffusion in the bulk (see Figure 6.4 for an illustration of bulk diffusion) and the ideal situation is no longer applicable. The atoms that move into the surface layer as a result of bulk diffusion originate from the first forty layers (see Terblans, et. al. [69] for a complete discussion). Also, it was mentioned in Chapter 4 that the bulk region must in effect be infinite (see section 4.2 of Chapter 4 for explanation) and therefore the bulk concentration cannot be affected by surface segregation. It would not be practical to construct a crystal with an enormously large crystal width, so instead the crystal width is further multiplied by 3. If one expresses all the conditions described above mathematically, the expression for the crystal width would be

$$\text{Crystal width} = \left(\frac{\text{maximum surface concentration}}{\text{bulk concentration}} \right) \times 2 \times 3 .$$

Using the above equation, the value for the crystal width used in this study was found to be

$$\begin{aligned} \text{Crystal width} &= \left(\frac{100\%}{2\%} \right) \times 2 \times 3 \\ &= 300 \text{ atoms.} \end{aligned}$$

Using the setup described at the beginning of this section, surface-segregation profiles were generated with the CPMC model. These profiles were compared to the values predicted by the well known Langmuir-McLean equation [2,57] (Figure 6.5), while the shapes of the kinetic part (short times) of the segregation profiles were compared to the shapes predicted by Fick's model. Finally these segregation profiles were also compared

with segregation profiles calculated with the modified Darken model [2,5,47,62], as shown in Figure 6.1-6.3.

6.3 Results and discussion

As mentioned in the previous section, various segregation and diffusion parameters were used to test the CPMC model. The first study was conducted using various diffusion coefficient (D_0) values.

6.3.1 CPMC and the diffusion coefficient

The profiles generated with the first three values listed in Table 6.1 are shown in Figure 6.1. Also shown in the inset are the calculated profiles obtained with the modified Darken and Fick model. The different diffusion coefficients had a marked influence on the rate at which segregation takes place. A smaller D_0 value leads to a slower surface segregation rate. The kinetic part of the CPMC model's segregation profiles follow the Fick model for a short time during the kinetic part of segregation [2,55]. The shape of the profiles is also similar to the modified Darken segregation profiles [69]. Run 2 was used as a reference for all the other runs that were performed

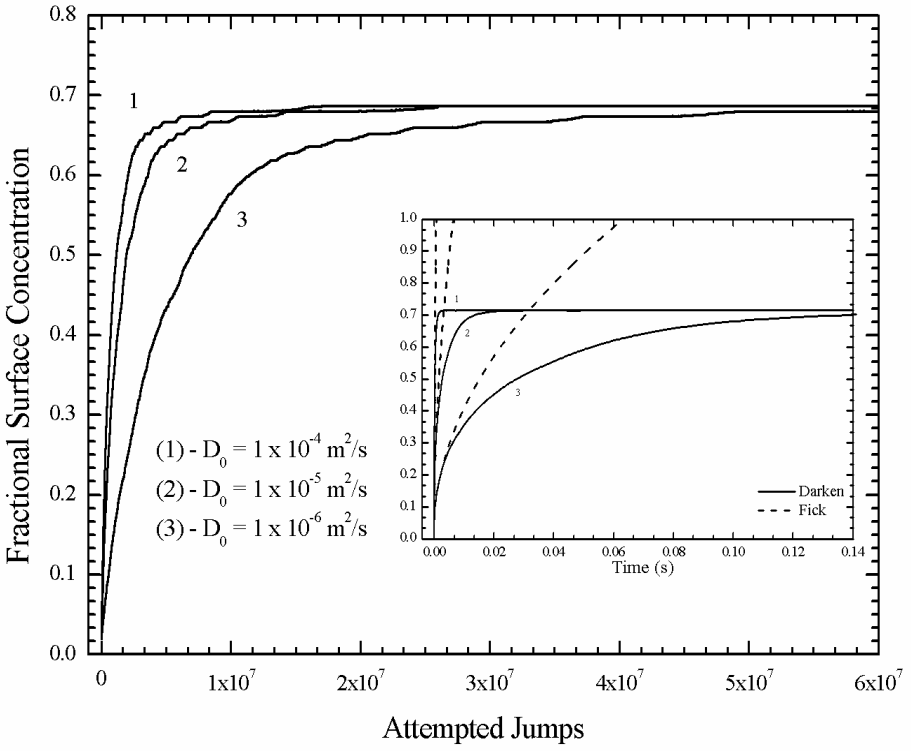

Figure 6.1: Segregation profiles calculated with the CPMC model using the following parameters: Q = 170 kJ/mol, T = 1000 K, X_B = 2 at%, ?G = -40 kJ/mol. The influence of the D_0 values can clearly be seen in the differing shape of the profiles. The inset graph shows the surface concentration vs time profiles as calculated with Fick's model and Darken's model [67].

Parameters	Run 1	Run 2	Run 3
ΔG_1 (kJ/mol)	-40	-40	-40
Q_1 (kJ/mol)	170	170	170
Q_2 (kJ/mol)	170	170	170
D_0 (solute element) (m^2/s)	1×10^{-4}	1×10^{-5}	1×10^{-6}
D_0 (solvent matrix) (m^2/s)	1×10^{-5}	1×10^{-5}	1×10^{-5}
Temperature (K)	1000	1000	1000

Table 6.1: Parameters used in the CPMC model calculations to study the effect that the diffusion coefficient has on the segregation profile.

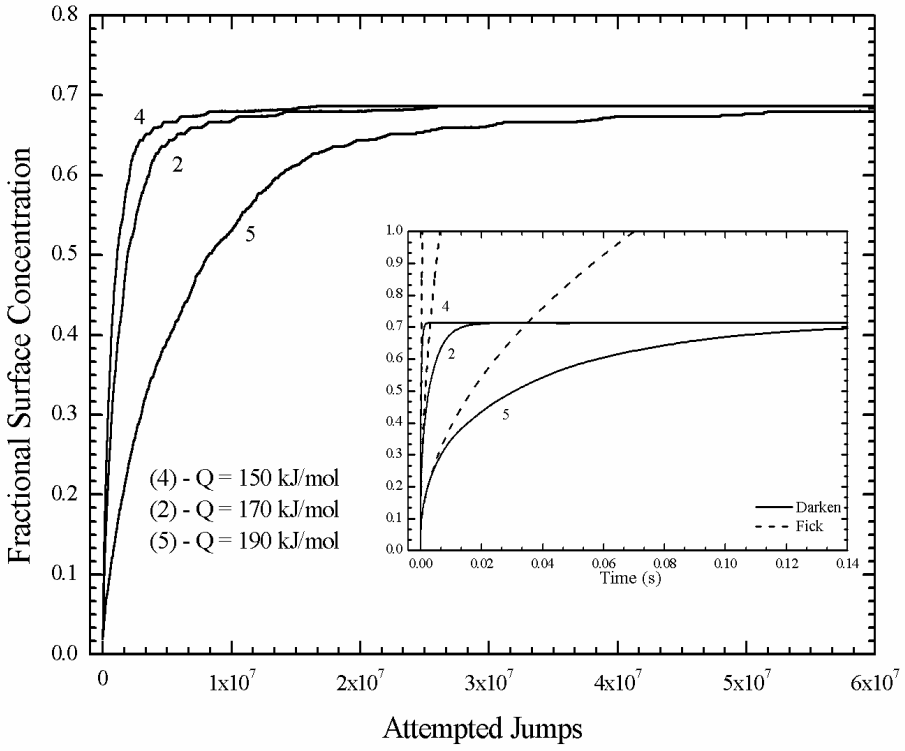

Figure 6.2: Segregation profiles calculated with the CPMC model using the following parameters: D_0 = 1×10^{-5} m^2/s, T = 1000 K, X_B = 2 at%, ?G = -40 kJ/mol. The influence of the Q values can clearly be seen in the differing shape of the profiles. The inset graph shows the surface concentration vs time profiles as calculated with Fick's model and Darken's model [67].

Parameters	Run 2	Run 4	Run 5
ΔG_1 (kJ/mol)	-40	-40	-40
Q_1 (kJ/mol)	170	150	190
Q_2 (kJ/mol)	170	170	170
D_0 (solute element) (m^2/s)	1×10^{-5}	1×10^{-5}	1×10^{-5}
D_0 (solvent matrix) (m^2/s)	1×10^{-5}	1×10^{-5}	1×10^{-5}
Temperature (K)	1000	1000	1000

Table 6.2: Parameters used in the CPMC model calculations to study the effect that the activation energy has on the segregation profile.

6.3.2 CPMC and the activation energy

A similar result is seen for the profiles generated with different activation energies (listed in Table 6.2), shown in Figure 6.2. Once again the rate at which atoms move to the surface is influenced. The smaller the activation energy, the more rapidly the atoms move into the surface. This is also in agreement with the infinite solution of Fick's equations as well as the modified Darken model.

6.3.3 CPMC and the segregation energy

Figure 6.3 shows the profiles generated for different segregation energies. The inset graph shows segregation profiles as calculated with the Darken model. The trend of the profiles generated by the CPMC model closely follows that of the Darken model. The CPMC model correctly predicted the equilibrium surface concentration for different segregation energies: a more positive ΔG leads to a lower surface concentration, in agreement with Darken's model.

Parameters	Run 2	Run 6	Run 7	Run 8
ΔG_1 (kJ/mol)	-40	-20	-30	-50
Q_1 (kJ/mol)	170	170	170	170
Q_2 (kJ/mol)	170	170	170	170
D_0 (solute element) (m^2/s)	1×10^{-5}	1×10^{-5}	1×10^{-5}	1×10^{-5}
D_0(solvent matrix) (m^2/s)	1×10^{-5}	1×10^{-5}	1×10^{-5}	1×10^{-5}
Temperature (K)	1000	1000	1000	1000

Table 6.3: Different values used for the segregation energy are listed. The profiles generated with these values will have different equilibrium surface concentration values.

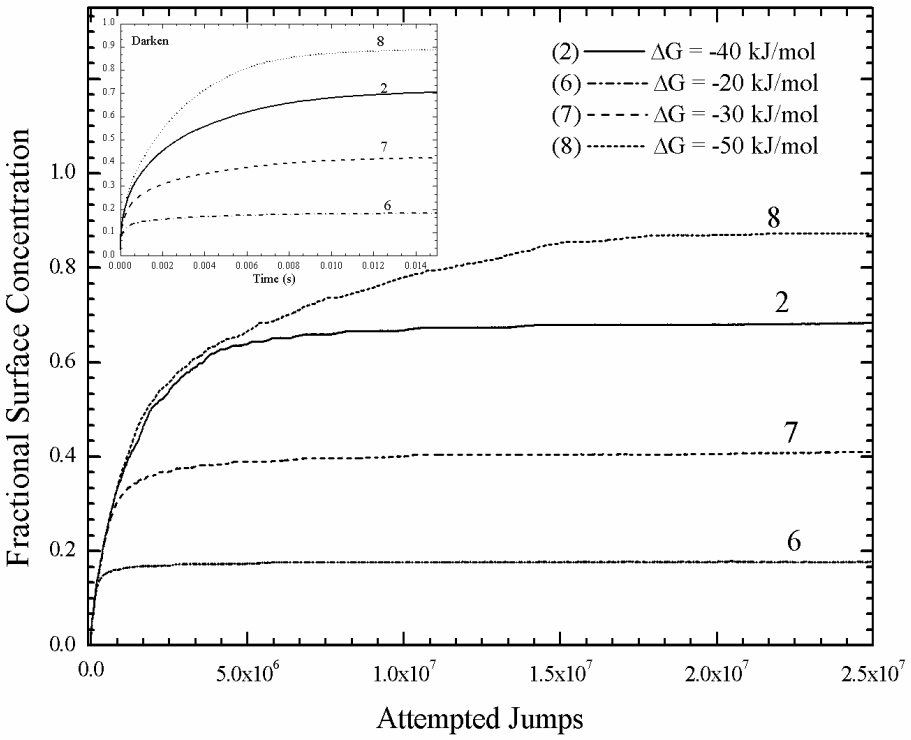

Figure 6.3: Segregation profiles calculated with the CPMC model using the following parameters: D_0 = 1×10^{-5} m^2/s, Q = 170 kJ/mol, T = 1000 K, X_B = 2 at%. Larger positive values for the segregation energy lead to lower equilibrium surface concentration profiles. The inset graph shows the equilibrium surface concentration vs time profiles generated with the Darken model [67].

Figure 6.4 shows the evolution of the depth profile of the crystal. Depletion of the immediate layers underneath the surface can clearly be seen in Figure 6.4. The layers underneath the surface return to the original bulk concentration after the surface layer has reached equilibrium; this is caused by the diffusion of atoms from deep in the bulk to the depleted layers.

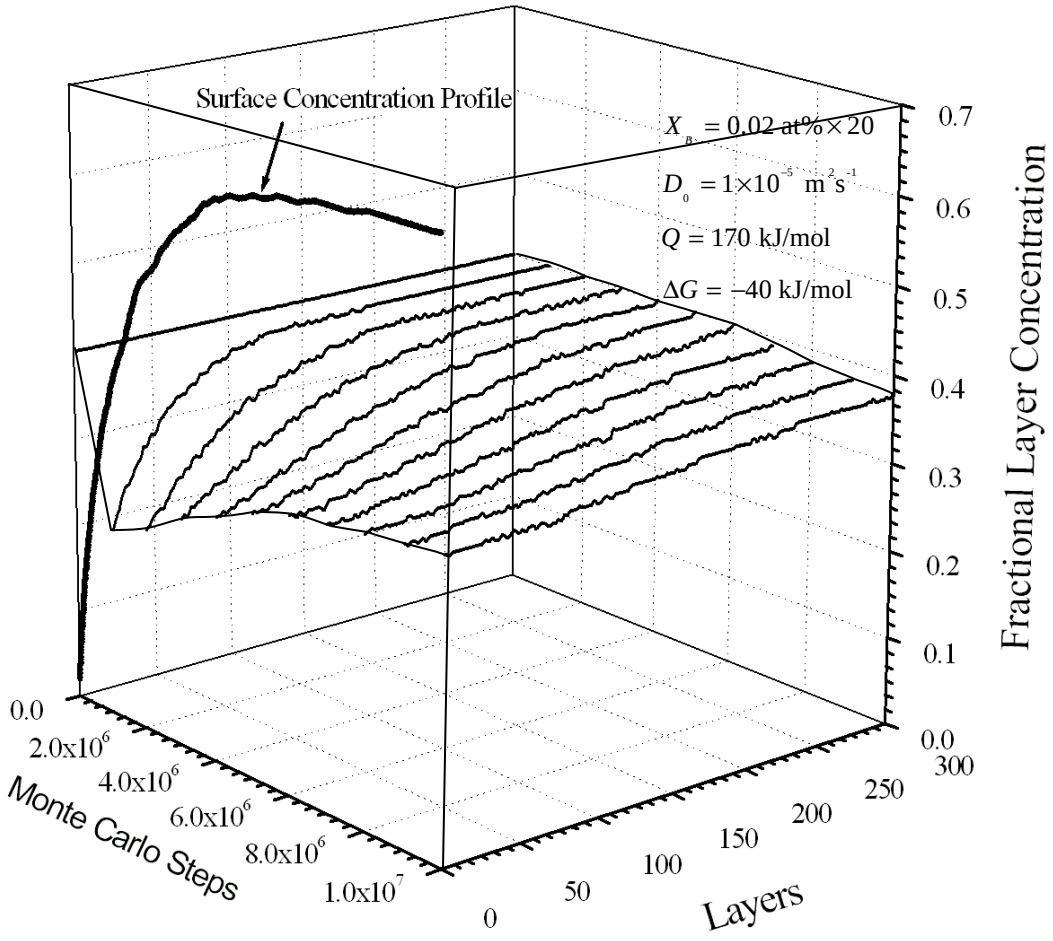

Figure 6.4: Representation of the evolution of the depth profile of the crystal. Depletion of the bulk region underneath the surface is visible in the figure. After the surface layer has reached equilibrium, this bulk region returns to the original bulk concentration by means of bulk diffusion. The bulk concentration in this figure was multiplied by a factor of 20 to improve visibility.

The equilibrium concentrations calculated the CPMC model are also compared to the equilibrium concentrations predicted by the Langmuir-McLean equation in Figure 6.5 [2,5,62]. From the figure it can be seen that the equilibrium concentrations calculated for different segregation energies closely match the form of the Langmuir-McLean curve.

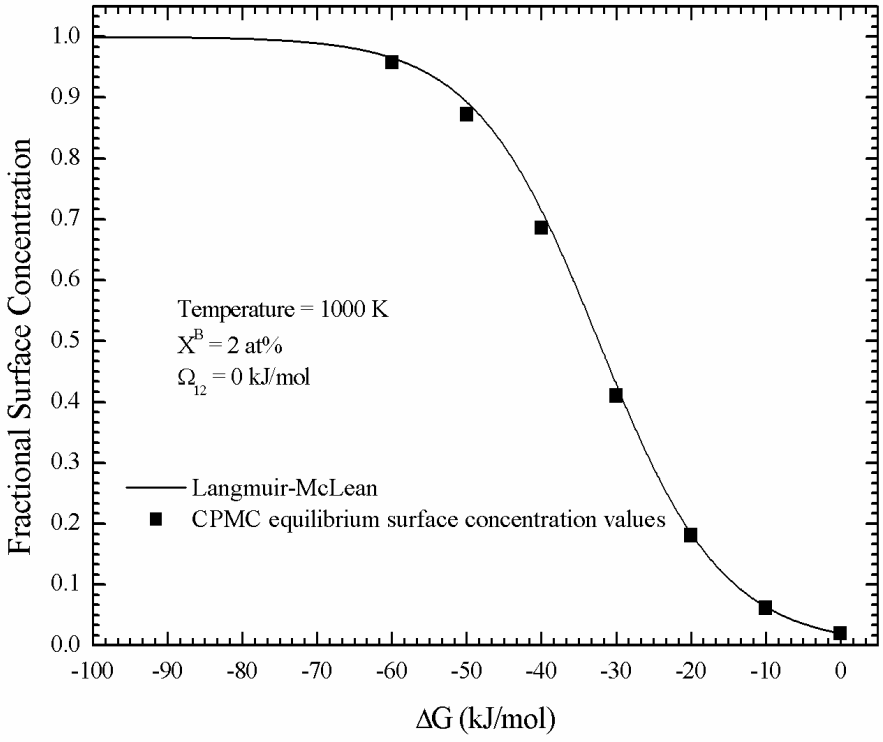

Figure 6.5: Comparison of the equilibrium surface segregation concentration and the equilibrium concentration values calculated with the Langmuir-McLean equation. The curve represents the equilibrium concentrations of the Langmuir-McLean equation while the squares represent the surface concentration values as calculated with the CPMC model. The CPMC model successfully predicted the equilibrium surface concentration values for differing segregation energies, as shown in this figure.

6.3.4 CPMC and parallel computing

The Achilles' heel of computational physics has always been the excessive time needed for calculations and simulations. Computational power has increased significantly in the last couple of decades, but there are still some calculations that require days or even weeks of computer time. One method of decreasing the computational time is to perform calculations in parallel. As mentioned in Chapter 1, the modified Darken model is difficult to implement in parallel, while the nature of the CPMC model allows easier parallel implementation.

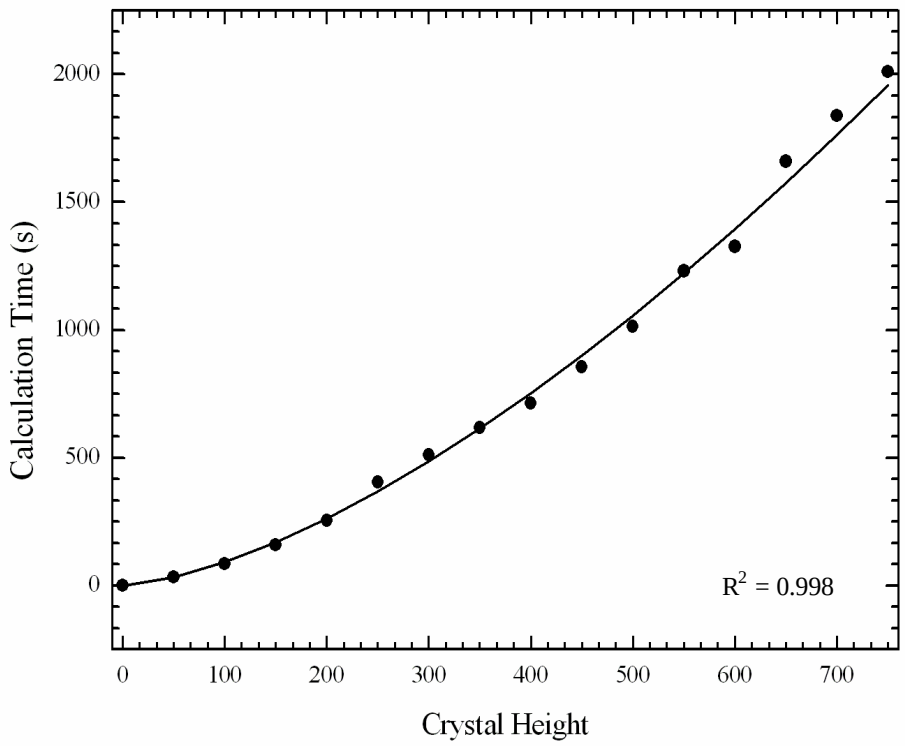

Figure 6.6: Illustration of the increase in actual computing time when the crystal height (and hence the total number of atoms) is increased. The width of the crystal in question was kept constant at 300 atomic layers. The calculation time shown is the time required for the surface layer to be 25 % covered.

Parallel implementation of the CPMC model is achieved by reducing the crystal height of the crystal being studied while keeping the crystal width constant. Figure 6.6 shows the increase in actual calculation time (with an increasing crystal height) to reach 25 % surface coverage. The increase is non-linear, with larger crystals requiring more computer time to perform the simulations.

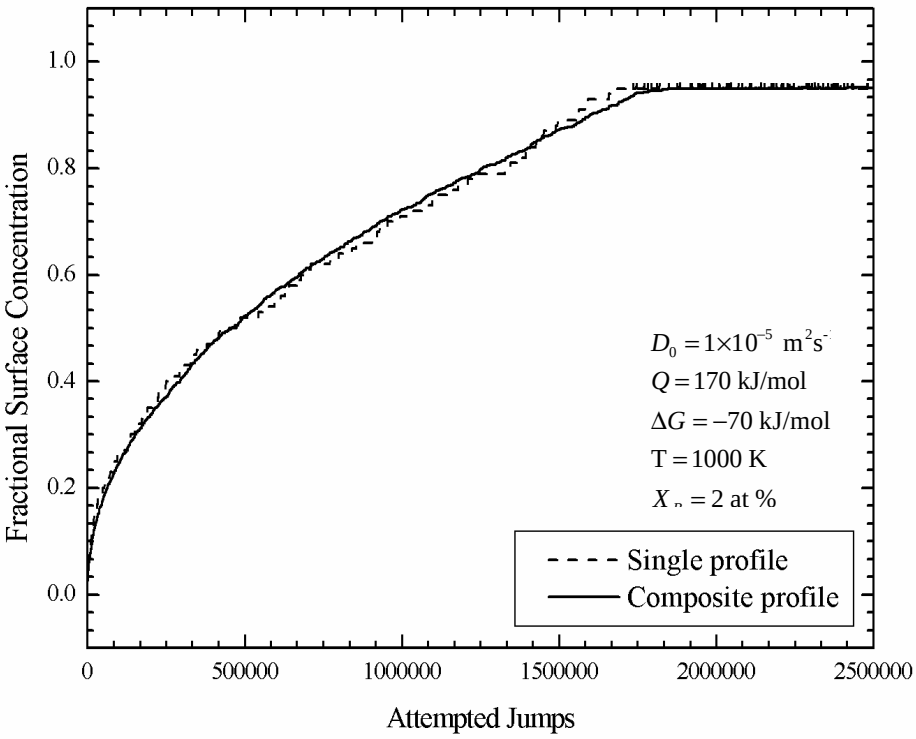

Figure 6.7: Illustration of the use of parallel computing to decrease the statistical noise on the segregation profiles. The dashed line represents the original segregation profile of the 100×300 crystal and the solid line represents the composite or average segregation profile obtained from ten crystals of size 100×300.

The parallel computing capability of the CPMC model was tested by performing calculations on 10 crystals, each having dimensions of 100×300. The segregation profile generated by the CPMC model for *one* crystal is shown is Figure 6.7 as the dashed line. A significant amount of statistical noise is visible on this profile. To improve the statistics of the segregation profile, the average of the ten parallel computed profiles was found and the result is shown as the solid line in Figure 6.7. Most of the statistical noise has been removed from the segregation profile while the shape of the profile has been improved dramatically.

The CPMC model is therefore capable of simulating surface-segregation and it is also easily implemented in a parallel environment. The CPMC-generated segregation profiles

also follow the trend of the profiles generated with the modified Darken model. On its own the CPMC model is not significantly faster than the modified Darken model, but a significant decrease in total calculation time is observed when the CPMC model is implemented in parallel.

Chapter 7

Conclusion and future work

7.1 Conclusion

A CPMC model that simulates surface segregation was successfully developed and implemented. A comparison was made between segregation profiles generated by the CPMC model and profiles generated with the existing modified Darken model as well as the Fick model. The result of the comparison show that segregation profiles obtained from the CPMC model follow the same trend as the profiles obtained for the modified Darken and Fick model. The model further also successfully simulated the kinetic as well as the equilibrium condition associated with surface segregation. The CPMC model was also successfully implemented in a parallel processing environment which enabled the rapid generation of segregation profiles from smaller crystals. The parallel generated profiles were added together and the statistical noise was reduced significantly.

When the equilibrium concentration values obtained from the CPMC model were compared to the values predicted by the Langmuir-McLean equation, it was found that the CPMC generated values closely follow the theoretical values.

The CPMC model is therefore a viable alternative to the existing segregation models.

7.2 Future work

The next step in the development of the CPMC is the extension of the calculation capabilities to include ternary and higher order alloys. Uniform concentration studies will continue, with bulk diffusion studies of thin layers playing a larger role. In addition to the uniform and thin layer systems, gas-induced segregation and diffusion is also a possible topic of investigation. A conversion of the attempted jumps shown in the figures in Chapter 6 to time will also be studied, since this will enable a direct comparison between experimental and generated profiles.

The development of a parallel software package will also receive some attention. A single computer will be able to control all the calculations and parameters that are performed in parallel. The software will also be able to import experimental data and perform the necessary theoretical fits on the experimental data.

Chapter 8

References

1 E. Christoffersen, P. Stoltze, J.K. N?rskov, *Surf. Sci* 505, 200 (2002)

2 J. du Plessis, *Solid State Phenomena – Part B, Volume 11, Diffusion and Defect Data*, Sci-Tech Publications, Brookfield USA (1990)

3 P. Wynblatt, A. Landa, *Comp. Mat. Sci.* 15, 250 (1999)

4 J.J. Terblans, W.J. Erasmus, E.C. Viljoen, J. du Plessis, *Surf. Interface Anal.* 22, 70 (1999)

5 E.C. Viljoen, J. du Plessis, H.C. Swart, G.N. van Wyk, *Surf. Sci.* 342, 1 (1995)

6 I.M. Sobol, *The Monte Carlo Method*, The University of Chicago Press, 1974

7 Symposium on Monte Carlo methods, University of Florida, 1954

8 J.M. Hammersley, D.C. Handscomb, *Monte Carlo Methods*, Methuen and Co., 1964

9 A. Doucet, N. de Freitas, N. Gordan, *Sequential Monte Carlo Methods in Practice*, Springer-Verlag New York, Inc., 2001

10 J.E. Gentle, *Random Number Generation and Monte Carlo Methods*, Springer-Verlag New York, Inc., 1998

11 Lj. Budinski-Petcovic, U. Kozmidis-Luburic, *Physica A* 301, 174 (2001)

12 A. Serra, R. Ferrando, *Surf. Sci.* 515, 588 (2002)

13 H. Li, F. Czerwinski, A. Zhilyaev, J.A. Szpunar, *Corrosion Science* 39 No. 7, 1211 (1997)

14 S. Artz, M. Shulz, S. Trimper, *Physics Letters A* 244, 271 (1998)

15 F. Szalma, W. Selke, S. Fischer, *Physica A* 294, 313 (2001)

16 R. Gorenflo, F. Mainardi, D. Moretti, G. Pagnini, P. Paradisi, *Physica A* 305, 106 (2002)

17 H. Ramalingam, M. Asta, A. Van De Walle, J.J. Hoyt, *Interface Science* 10, 149 (2002)

18 V. Konakov, E. Mammen, *Stochastic Processes and their Applications* 96, 73 (2001)

19 Y. Kangawa,, T. Ito, A. Taguchi, K. Shiraishi, T. Irisawa, T. Ohachi, *App. Surf. Sci.* 190, 517 (2002)

20 P. Deurinck, C. Creemers, *Surf. Sci.* 419, 62 (1998)

21 Hanchen Huang, G.H. Gilmer, *Journal of Computer-Aided Materials Design* 6, 117 (1999)

22 M. Kaukonen, J. Peräjoki, R. M. Nieminen, *Physical Review B* 61 No. 2, 980 (2000)

23 R. Weinkamer, P. Fratzl, B. Sepiol, and G. Vogl, *Physical Review B* 58 No. 6, 3082 (2000)

24 S. De, S. Teitel, Y. Shapir, E. H. Chimowitz, *J. Chem. Phys.* 116 No. 7, 3012 (2002)

25 M. Castier, O.D. Cuéllar, F.W. Tavares, *Powder Technology* 97, 200 (1998)

26 H. Deng, W. Hu, X. Shu, L. Zhao,B. Zhang, *Surf. Sci.* 517, 177 (2002)

27 B. Zheng, *Physica A* 283, 80 (2000)

28 T.C. Kinga;, Y.K. Kuob, M.J. Skovec, *Physica A* 313, 427 (2002)

29 E.C. Mbamala, G. Pastoreb, *Physica A* 313, 312 (2002)

30 B. Hetényi, E. Rabani, B. J. Berne, *J. Chem. Phys.* 110, No 13, 6143 (1999)

31 Lj. Budinski-Petkovic, U. Kozmidis-Luburic, A. Mihailovic, *Physica A* 293, 339 (2001)

32 H. Mizuseki, K. Hongo1, Y. Kawazoe1, L.T. Wille, *Scripta mater.* 44, 1911 (2001)

33 S.A. Rice, M. Zhao, *Physical Review B* 57 No. 21, 13501 (1998)

34 G.S. Bokun, Y.G. Groda, C. Uebing, V.S. Vikhrenko, *Physica A* 296, 83 (2001)

35 B. Good, G. Bozzolo, *Surf. Sci.* 507–510, 730 (2002)

36 J.P. Muscat, *J. Phys. C: Solid State Phys.* 15, 867 (1982)

37 B. Good, G.H. Bozzolo, P.B. Abel, *Surf. Sci.* 454–456, 602 (2000)

38 D.R. Askeland, *The Science and Engineering of Materials*, 3rd S.I. edition, Stanly Thornes Publishers, 1998

39 B. Tuck, *Introduction to diffusion in semiconductors*, IEE Monograph Series 16, Peter Peregrinus Ltd., 1974

40 J. du Plessis, P.E. Viljoen and G.N. van Wyk, *Surf. Sci.* 244, 277-284, 1991

41 A.G. Guy, *Introduction to Material Science*, McGraw-Hill Kogakusha, 1972

42 S. Elliot, *The Physics and Chemistry of Solids*, John Wiley and Sons, 1998

43 R.J. Borg, G.J. Dienes, *An Introduction to Solid State Diffusion*, Boston Academic Press, 1988

44 H.P. Meyers, *Introductory Solid State Physics*, 2nd Edition, Taylor and Francis, 1997

45 M.A. Omar, *Elementary solid state physics: principles and applications*, 1st edition, Addison-Wesley, 1975

46 P.G. Shewmon, *Diffusion in Solids*, McGraw-Hill Book Company, 1963

47 J. du Plessis, G.N. van Wyk, *J. Phys. Chem. Solids* 49 No. 12, 1441 (1988)

48 W.J. Erasmus, *Die segregasie van Sb na die lae indeksoppervlakke van Cu enkelkristalle*, MSc Thesis, University of the Free State, South Africa (1999)

49 J.Y. Wang, J. du Plessis, J.J. Terblans and G.N. van Wyk, *Surf. Sci.* 423, 12-18, 1999

50 J. du Plessis, G.N. van Wyk, *J. Phys. Chem. Solids* 50 No. 3, 247 (1989)

51 E.C. Viljoen, *Lineêre verhittingstudies van oppervlaksegregasie in binêre allooie*, PhD thesis, University of the Free State, South Africa (1995)

52 J. du Plessis, G.N. van Wyk and E. Taglauer, *Surf. Sci.* 220, 381-390, 1989

53 J.Y. Wang, J. du Plessis, J.J. Terblans and G.N. van Wyk, *Surf. Interface Anal.* 28, 73-76, 1999

54 J.J. Terblans, W.J. Erasmus, E.C. Viljoen and J. du Plessis, *Surf. Interface Anal.* 28, 70-72, 1999

55 J. du Plessis and E.C. Viljoen, *App. Surf. Sci.* 100-101, 222, 1996

56 J. du Plessis and E.C. Viljoen, *App. Surf. Sci.* 59, 171, 1992

57 J. du Plessis, G.N. van Wyk, *J. Phys. Chem. Solids* 50 No. 3, 237 (1989)

58 P.E. Viljoen, J. du Plessis, F. Bezuindenhout, *J. Vac. Sci. Tech. A* 5 No. 4, 1015 (1987)

59 J. du Plessis, *S. Afr. J. Phy.* 1/2, 31 (1992)

60 E.C. Viljoen, J. du Plessis, *Surf. Interface Anal.* 22, 598 (1994)

61 E.C. Viljoen, J. du Plessis, *Surf. Interface Anal.* 23, 110 (1995)

62 J.J. Terblans, W.J. Erasmus, E.C. Viljoen, J. du Plessis, *Surf. Interface Anal.* 22, 70 (1999)

63 J.Y. Wang, J. du Plessis, J.J. Terblans, G.N. van Wyk, *Surf. Interface Anal.* 28, 73 (1999)

64 J. du Plessis, *Surf. Sci.* 287/288, 857 (1993)

65 J. du Plessis, P.E. Viljoen, G.N. van Wyk, *Surf. Sci.* 244, 277 (1991)

66 J. du Plessis, *App. Surf. Sci.* 70/71, 303 (1993)

67 D.A. Porter, K.E. Easterling, *Phase Transformations in Metals and Alloys*, Chapman & Hall, (1981)

68 C.H.P. Lupis, *Chemical Thermodynamics of Materials*, North-Holland, Amsterdam, 1983

69 J.J. Terblans, *Modelling and experimental investigation of Sb-surface segregation in Cu-single crystals*, PhD Thesis, University of the Free State, South Africa (2001)

Conference contributions and publications

1. **A Monte Carlo program for simulating segregation and diffusion utilizing chemical potential calculations**
   Joubert, H.D., Swart, H.C., Terblans, J.J.
   2nd International Conference of the African Materials Research Society
   2003
   Page 210

2. **A Monte Carlo program for simulating segregation and diffusion utilizing chemical potential calculations**
   Joubert, H.D., Swart, H.C., Terblans, J.J.
   Surface and Interface Analysis
   Accepted 16 April 2004

3. **A Chemical Potential Monte Carlo (CPMC) program for simulating diffusion and segregation**
   Joubert, H.D., Swart, H.C., Terblans, J.J.
   SAIP Conference
   2004